THE HOROMAN PERIDOTITE COMPLEX, JAPAN: THE UPPER MANTLE VARIATIONS IN ONE PLACE

Tomoaki Morishita[*,**,✉] and **Eiichi Takazawa**[**,****,✉]

* *School of Geosciences and Civil Engineering, Kanazawa University, Volcanoes and Earth's Interior Research Center, Kanazawa, Japan.*

** *Research Institute for Marine Geodynamics, Japan Agency for Marine-Earth Science and Technology, Yokosuka, Japan.*

*** *Department of Geology, Faculty of Science, Niigata University, Niigata, Japan.*

✉ *Corresponding authors, email: tomo_make_a_wish@icloud.com, takazawa@geo.sc.niigata-u.ac.jp*

Keywords: *Melting-Melt extraction; Metasomatism; P-T trajectory; Mafic rocks; Isotopic composition.*

ABSTRACT

The spectrum of ultramafic and mafic rocks in the Horoman Peridotite Complex provides a near-perfect natural laboratory to study the process of melt generation, mixing of crustal component, melt-rock interaction, metasomatism and deformation in the mantle and/or during exhumation. It physically preserves the so-called "source rock" (lherzolite), the residue after partial melting (harzburgite), and the crystallized melts (ultramafic and mafic rocks) all in one place, allowing earth scientists to directly observe the consequences of a fundamental planetary process. Based on a synthesis of extensive research findings and our field observations, the Horoman Peridotite Complex is interpreted to have formed as follows: The incipient petrogenetic stage at approximately 1 Ga involved polybaric partial melting of a mid-ocean ridge basalt (MORB)-source mantle during its ascent across the garnet-spinel facies boundary, generating a heterogeneous residual suite (the Main Harzburgite-Lherzolite Suite: MHL) that was accompanied by the crystallization of gabbroic protoliths for the second major mafic layers (Type II mafic layer) with cumulus ultramafic rocks (the Spinel-rich Dunite-Wehrlite suite: SDW). Following their initial formation in the shallow oceanic lithosphere, the MHL and SDW suites including the Type II mafic layer underwent profound tectonic burial into the garnet peridotite stability field. The Banded Dunite-Harzburgite (BDH) suite, which is a product of high-Mg andesitic magmatism in an arc setting, was incorporated as exotic blocks. Subsequently, the integrated lithological framework was intruded by melts for the formation of the most abundant mafic layer and the third most abundant rock (Type I and minor Type III mafic layers), which crystallized as garnet pyroxenites. This entire assemblage then underwent tectonic ascent – potentially as a mantle diapir – transitioning from the garnet- to the plagioclase-peridotite stability field. During this exhumation, melt-rock interactions at approximately 50 Ma facilitated the formation of mega-olivine dunite channels, while localized partial melting and melt segregation within the MHL suite yielded characteristic plagioclase-rich veins. Multi-stage metasomatic events driven by the infiltration of slab-derived fluids impacted all lithological units and facilitated the localized crystallization of hydrous phases, specifically phlogopite and pargasite, at ca. 23 Ma. While late-stage processes have overprinted much of the complex, the MHL plagioclase peridotite uniquely preserves isotopic signatures of ancient depletion dating back to 1 Ga. These results provide a comprehensive model for the tectonic transport of mantle lithologies from mid-ocean ridge environments to subduction zones.

INTRODUCTION

The Horoman Peridotite Complex, located in Samani Town, Hokkaido, Japan, has been widely recognized as an ultramafic body exhibiting extremely low serpentinization, displaying diverse lithologies ranging from dunite to lherzolite, including pyroxenite and "gabbroic" layers (e.g., Igi, 1953; Nagasaki, 1966; Komatsu and Nochi, 1966; Niida, 1974, 1975b, 1984) (Note that, as will be introduced later, gabbroic rocks are metamorphosed mafic rocks; however, in the early stages of research on the Horoman Peridotite Complex, they were referred to as gabbroic rocks).

In 1992, two important papers on the Horoman Peridotite Complex were published in the same volume of Nature (Takahashi, 1992; Takazawa et al., 1992). Since then, the Horoman Peridotite Complex has been studied from numerous geochemical and structural perspectives as demonstrated in this paper. The ultramafic and mafic lithologies of the Horoman Peridotite Complex record a complex petrogenetic history involving partial melting, melt-rock interaction, metasomatism and metamorphism under dynamic P-T conditions. Although numerous age constraints have been reported for these events, significant discrepancies sometimes exist among the suggested ages (Akizawa et al., 2021).

There are three excellent Japanese-language reviews on the Horoman Peridotite Complex (Niida and Takazawa, 2007; Akizawa et al., 2021; Matsuyama and Michibayashi, 2025). Niida and Takazawa (2007) was prepared as a field guide for a post-conference meeting of the Geological Society of Japan and presented basic information and key research findings regarding the Horoman Peridotite Complex. Akizawa et al. (2021) conducted a detailed examination of the relationships between isotopic age data and melting/metasomatic events, and identified reliable isotopic age data. Furthermore, by combining these isotopic age data with interpretations of undated events, they presented a potential model of pressure-temperature-deformation-time history of the Horoman Peridotite Complex. Matsuyama and Michibayashi (2025) summarized the results of microstructural observations aimed at elucidating the deformation history and rheological aspects of the Horoman peridotites and discussed their relationship to the geological development of the surrounding region. Although these papers overlap with those in many aspects, we have aimed to synthesize the findings of numerous previous studies and to include several geological observations that we consider important for all researchers to keep in mind in further studies of the Horoman Peridotite Complex. We understand that our observations and interpretations are not fully accepted by other researchers. However, it is hoped that this paper will contribute to researchers finding new interests in the Horoman Peridotite Complex. This paper cannot provide a detailed introduction to the relationship between the Horoman Peridotite Complex and the surrounding rocks as well as geophysical observations such as

gravity (Yamamoto et al., 2001), seismic velocity (Arita et al., 1998, Tsumura et al., 1999) and electric resistivity (Ichihara et al., 2016), nor to the tectonic evolution during the final uplift process with the surrounding rocks. For discussions on these topics, please refer to the relevant topics in Niida (1974), Komatsu (1982), Sawaguchi (2004), Yamamoto et al. (2010), Matsuyama and Michibayashi (2023, 2024), Tasaka et al. (2024) and the references therein.

GEOLOGICAL OUTLINE

The Horoman Peridotite Complex is exposed at the southern end of the Main Zone of the Hidaka metamorphic belt in Hokkaido, Japan (Komatsu et al., 1982; Niida, 1984). The high-T/P Hidaka metamorphic belt is interpreted as an exhumed, ~23-km-thick cross-section of crustal sequence of magmatic arc (Komatsu et al., 1984; Osanai et al., 1992). Several peridotite bodies (Uenzaru-Pankenushi (the eastern part), Horoman, Nikanbetsu and Abeyaki bodies) occur at the basal zone of the Main Zone (Komatsu et al., 1982; Niida and Takazawa, 2007). The Horoman Peridotite Complex, which is the largest body of them, forms an approximately 8 × 10 km body, with a maximum thickness of 3-4 km (Fig. 1) (Komatsu and Nochi, 1966; Niida, 1974, 1984; Sawaguchi, 2004).

To contextualize the origin and evolution of the Horoman Peridotite Complex, the discussion focuses on two key characteristics: its subdivision into the Upper and Lower Zones, and the occurrence of symplectitic mineral aggregates. Both features are fundamentally linked to the overarching petrogenetic evolution of the complex.

The Upper and Lower Zones

The Horoman Peridotite Complex is subdivided into the Upper Zone (about 1 km in thickness) and the Lower Zone (about 2 km in thickness) based on distinct lithological and textural contrasts (Komatsu and Nochi, 1966; Niida, 1974, 1984; Ozawa and Takahashi, 1995, Matsukage and Arai, 1996; Yoshida and Takahashi, 1997; Takahashi, 1997, 2001) (Fig. 1). The Upper Zone is predominated by plagioclase peridotite. In contrast, the Lower Zone is characterized by a predominance of spinel lherzolite and harzburgite over plagioclase lherzolite (Figs. 1, 2 and 3). The Upper Zone features more frequent mafic layers (called gabbros in earlier papers) that alternate with peridotite, and these layers possess sharper boundaries compared to those in the Lower Zone (Figs. 2 and 3). The Upper Zone contains plagioclase-rich veins (Fig. 3). These veins are completely absent in the Lower Zone. The difference between the Upper Zone and the Lower Zone is a

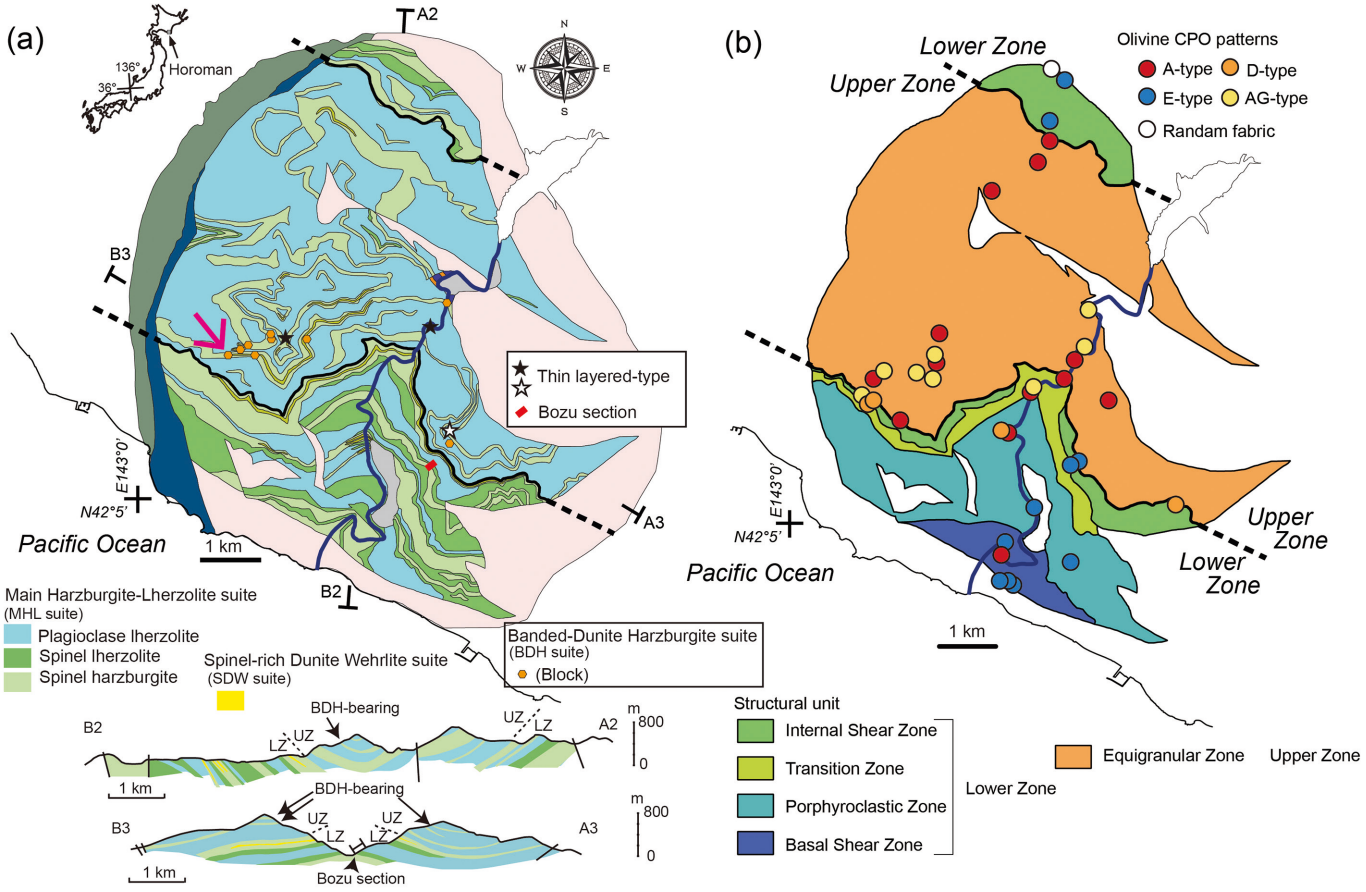

Fig. 1 - Lithological map (a) and structural unit map (b) of the Horoman Peridotite Complex after Sawaguchi (2004). (a) Representative cross-sections of A2-B2 and A3-B3 are shown. The map illustrates the spatial distribution and field relationships between the main suites (Main Harzburgite-Lherzolite suite and Spinel-rich Dunite Wehrlite suite) (MHL-SDW) and the exotic BDH blocks. Key localities are indicated, marking critical exposures that constrain the petrogenetic relationships. Solid black stars indicate typical outcrops of Thin layered-type plagioclase peridotite alternating with mafic layers studied by Toramaru et al. (2001), Tasaka et al. (2024) and Malaviarachchi et al. (2008, 2010). White star is the outcrop on the western ridge of Bozu-yama, as described by Toramaru et al. (2001). Pink arrow indicates the "Nanagome" outcrop demonstrating the complex spatial relationships between the MHL-SDW suite and the exotic BDH blocks. (b) The locations where Matsuyama and Michibayashi (2023) obtained the crystal preferred orientation (CPO) patterns of olivine are shown on the map.

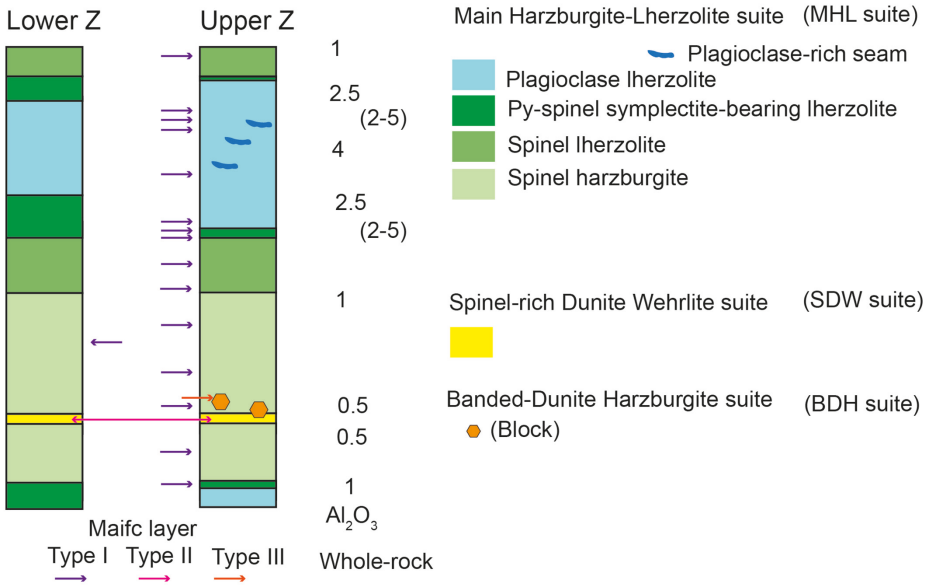

Fig. 2 - Schematic lithological successions illustrating the layered structure of the Lower and Upper Zones in the Horoman Peridotite Complex. The MHL harzburgite hosts the SDW suite and associated Type II mafic layers. Type III mafic layer is rare and occurs in an exotic BDH block. In contrast, Type I mafic layers are predominantly hosted within the MHL suite. The Upper Zone is distinguished by higher frequency of Type I mafic layers and the occurrence of "Thin layered-type plagioclase peridotite", consisting of centimeter-scale alternation of mafic and ultramafic rocks. While the whole-rock compositions of schematic successions are assumed to be mutually consistent, the Upper Zone records a high temperature trajectory that facilitated the partial melting of fertile peridotites and mafic layers that formed plagioclase-rich seams. This fundamental lithological succession repeats cyclically throughout the complex.

unique characteristic of the Horoman Peridotite Complex and has been discussed by several aspects.

Symplectitic mineral aggregate

The presence of symplectite is one of the characteristic features of the Horoman Peridotite Complex (Kushiro and Yoder, 1966; Takahashi and Arai, 1989; Ozawa and Takahashi, 1995; Takazawa et al., 1996; Morishita and Arai, 1997; Morishita et al., 2003) (Fig. 4). Symplectite is a microtexture characterized by intergrowth of two or more minerals with vermicular shape. The vermicular intergrowths of the Horoman symplectites has gathered significant attention (Morishita and Obata, 1995; Obata, 1997; Morishita, 1998; Odashima et al., 2008), particularly regarding the reaction kinetics governing their formation, as shown in the Supplementary Material.

Symplectites in the Horoman Peridotite Complex are classified into two types based on their mineral assemblage (Niida, 1984; Takahashi and Arai, 1989; Ozawa and Takahashi, 1995; Morishita and Arai, 1997): two-pyroxene (orthopyroxene and clinopyroxene) and aluminous spinel symplectite (pyroxene-spinel symplectite, hereafter), and plagioclase-bearing symplectite (plagioclase symplectite, hereafter), which is characterized by plagioclase around fine-grained spinel, sometimes exhibiting a vermicular shape (Takahashi and Arai, 1989; Ozawa and Takahashi, 1995; Morishita and Arai, 1997) (Fig. 4). The pyroxene-spinel symplectite is generally enclosed by a fine-grained (100-200 μm) mineral aggregate (lenticular seam). The mineral grain size and mineral composition of symplectite in the Upper Zone are coarser and more homogeneous than those in the Lower Zone (Ozawa and Takahashi, 1995; Morishita and Arai, 2003). The Horoman symplectite is interpreted as a subsolidus decompression reaction product of garnet during the ascent of the complex, as presented below.

Another scientific objective using the Horoman peridotites with a low degree of serpentinization

An ultramafic pseudotachylyte-like vein and a serpentinized cataclastic peridotite was reported by Morishita (1998, 2000a). These rocks can provide unique insights into the brittle deformation of peridotite, as the Horoman peridotite complex has undergone only extremely minor serpentinization. Fresh peridotite samples from the Horoman Peridotite Complex are used as geochemical standard samples (Miura and Nagano, 1991; Imai et al., 1995; Mikuni et al., 2025). Using these fresh Horoman peridotite and gabbroic samples, unique findings regarding physical properties (dilatancy phenomena) have been reported through high precision triaxial deformation experiments (Akamatsu et al., 2019).

PETROLOGICAL DIVERSITY

Three different Suites for peridotites

Detailed petrological work revealed that the Horoman Peridotite Complex comprises three distinct peridotite suites: (1) The Main Harzburgite-Lherzolite Suite (MHL), (2) Spinel-rich Dunite-Wehrlite Suite (SDW), and (3) the Banded Dunite-Harzburgite suite (BDH) (Takahashi, 1991, 1992) (Figs. 1 and 2, Table 1). First, we briefly introduce these three peridotite suites. The lithological classification and age data for the Horoman Peridotite Complex are summarized in Tables 1 and 2.

The MHL suite occupies the main part of the Complex and consists of harzburgite, spinel lherzolite, and plagioclase lherzolite, forming a layered complex with gradual boundaries in mineral mode (Fig. 2). Mineral chemistry of the MHL suite shows a wide compositional range; as the proportion of modal pyroxene decreases, the Fo content of olivine and the Cr# (the atomic ratio of Cr to (Cr+Al)) of discrete spinel increase (Fig. 5).

Plagioclase peridotites of the MHL suite exhibit diversity, and their origins are key to understanding the evolution of the Horoman Peridotite Complex. The origin of plagioclase peridotite in the Upper Zone needs to be discussed in relation to mafic rocks. To make the following explanation easier to understand, we now provide a brief overview of varieties of the MHL plagioclase peridotite. Plagioclase peridotites of the MHL suite can be classified into three petrogenetic types by integrating previous studies (Type I/II of Yoshida and Takahashi, 1997; N/E-types of Takazawa et al., 2000, DP/EP types of Yoshikawa and Nakamura, 2000, and TLP/MSP

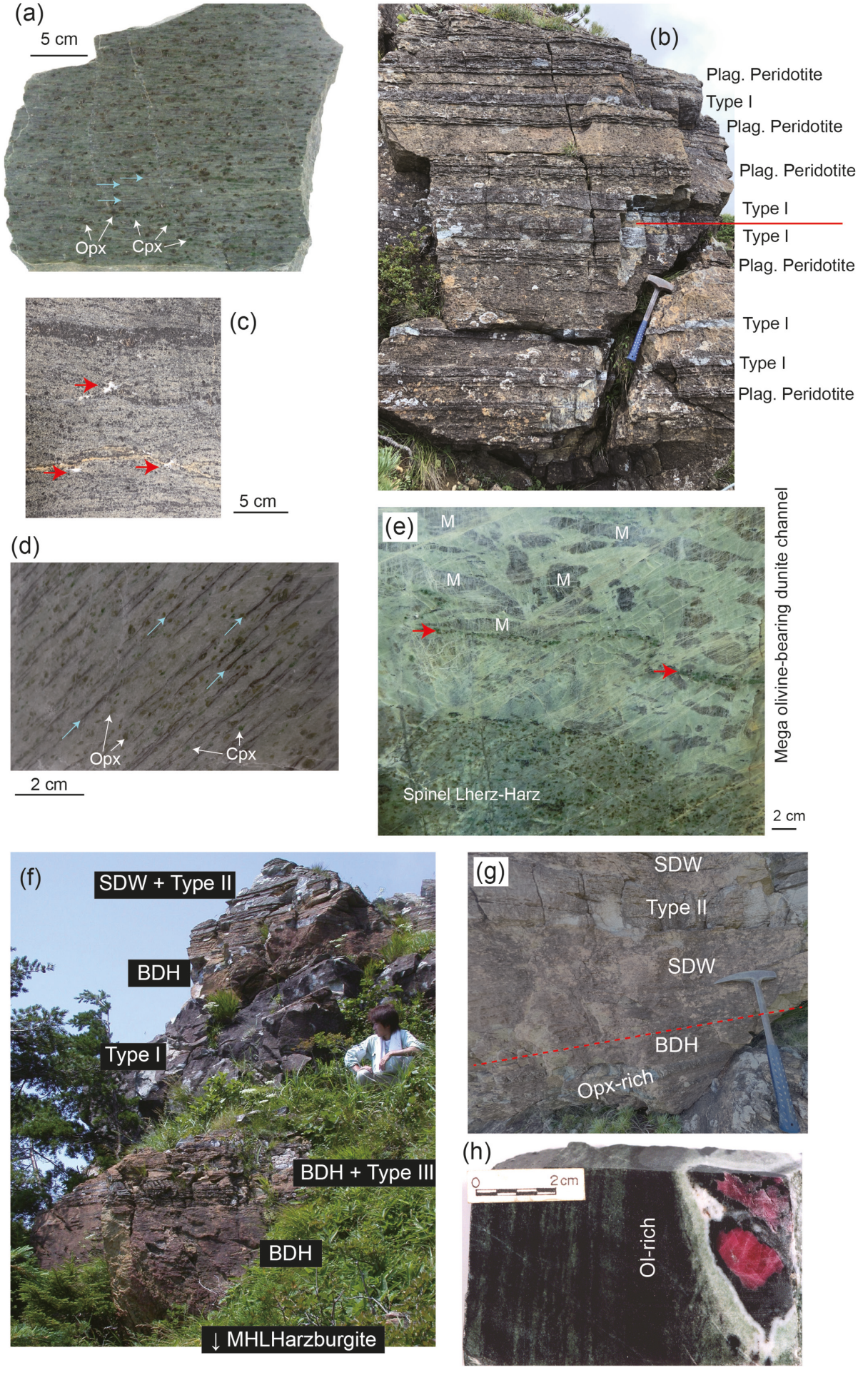
(a)
5 cm
Opx
Cpx
(b)
Plag. Peridotite
Type I
Plag. Peridotite
Plag. Peridotite
Type I
Type I
Plag. Peridotite
Type I
Type I
Plag. Peridotite
(c)
5 cm
(d)
Opx
Cpx
2 cm
(e)
M
M
M
M
M
Spinel Lherz-Harz
Mega olivine-bearing dunite channel
2 cm
(f)
SDW + Type II
BDH
Type I
BDH + Type III
BDH
↓ MHLHarzburgite
(g)
SDW
Type II
SDW
BDH
Opx-rich
(h)
0
2 cm
Ol-rich

Fig. 3 - Representative rock samples and field occurrences of the Horoman Peridotite Complex. (a) Plagioclase lherzolite of the MHL suite (Lower Zone). Light blue arrows highlight fine-grained mineral aggregates containing plagioclase, which represent pseudomorphs after precursor garnet formed during exhumation from garnet- to plagioclase-peridotite stability conditions. (b) Thin-layered plagioclase peridotite and Type I mafic layers. This outcrop features the "Thin-layered type" (see text) characterized by centimeter-scale alternations of plagioclase peridotite and mafic layers. The red line marks the "symmetrical center" identified by Toramaru et al. (2001). (c) Plagioclase-rich seams in the MHL plagioclase lherzolite (Upper Zone). Red arrows indicate plagioclase-rich seams. These features crosscut the primary foliation and are interpreted as products of localized partial melting during the late-stage ascent under plagioclase peridotite conditions. (d) Symplectite-bearing lherzolite of the MHL suite (Lower Zone). Light blue arrows indicate fine-grained mineral aggregates including pyroxene-spinel symplectites, which serve as evidence for the breakdown of garnet. (e) Mega olivine-bearing dunite channel within the MHL spinel lherzolite-harzburgite (Lower Zone). These channels are interpreted to have formed via intensive melt-rock interaction at approximately 50 Ma (Yoshikawa et al., 2019). (f) Overview of the Nanagome outcrop. This key locality demonstrates the complex spatial relationships between the MHL-SDW framework and the exotic BDH blocks. Visible components include the SDW suite with Type II mafic layers, the BDH suite with Type III mafic layers, and Type I mafic layers. (g) Direct contact between the SDW and BDH suites. The red dashed line delineates the boundary between the SDW suite (interlayered with Type II mafic layers) and the BDH suite. This contact provides critical evidence that the BDH blocks were incorporated into the complex after the initial formation of the MHL-SDW suites. (h) Corundum-bearing Type II mafic layer. The pinkish corundum, which existed as a stable phase under eclogite-facies conditions prior to exhumation of the Horoman Peridotite complex. The layering consists of dark olivine-rich bands and dark-green clinopyroxene-rich bands.

types of Malaviarachchi et al., 2008, 2010; Ranaweera et al., 2018) (Figs. 6 and 7).

1) Normal-type plagioclase peridotite is characterized by fertile major element compositions (high Al_2O_3 and CaO) yet are markedly depleted in light rare earth elements (LREEs) and exhibit depleted isotopic signatures (high $^{143}Nd/^{144}Nd$ and low $^{87}Sr/^{86}Sr$).
2) Enriched-type plagioclase peridotite highlights a profound geochemical decoupling: major element depletion (refractory, such as low Al_2O_3 and CaO compared to Normal-type) contrast with cryptic enrichment in incompatible elements and radiogenic isotopes (low $^{143}Nd/^{144}Nd$ and high $^{87}Sr/^{86}Sr$).
3) Thin-layered-type plagioclase peridotite is interlayered with Type I mafic layers (the major mafic rock of the Horoman Complex described below) on a millimeter-to-centimeter scale (Fig. 3b). A distinguishing geochemical feature of the Thin-layered-type is that its clinopyroxene exhibits high Al and REE concentrations respect to the other types.

The SDW suite, mainly composed of spinel-rich dunite and wehrlite, occurs as layers within harzburgite of the MHL suite (Figs. 1 and 2), typically with sharp boundaries in mineral mode and chemistry, and reaches thickness of up to 15 m. This basic succession repeats several times in the complex (Fig. 1) (Takahashi, 1991, 1992). Fo content of olivine of the SDW suite is significantly lower than that of other peridotite groups, while the TiO_2 content of spinel is relatively high (Fig. 5).

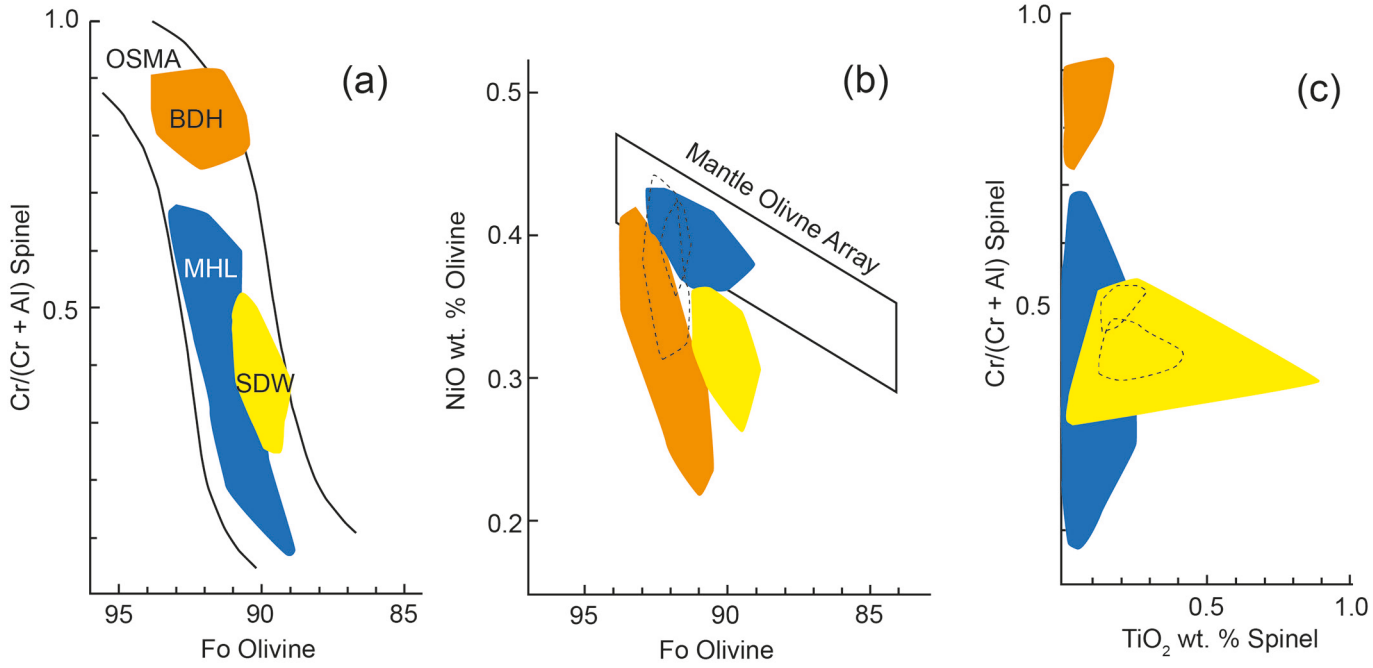

Fig. 4 - Microtextural evidence for the decompression from garnet peridotite stability conditions of the MHL suite: symplectite. Symplectitic mineral aggregates represent pseudomorphs after precursor garnet, recording the tectonic ascent of the Horoman Complex from garnet peridotite to plagioclase peridotite stability conditions. (a, b) Photomicrographs of fine-grained mineral aggregates containing pyroxene-spinel symplectites from the Lower Zone and Upper Zone, respectively. Pink arrows indicate the symplectite domains within the fine-grained mineral aggregates. (c, d) Back-scattered electron (BSE) images providing details of the pyroxene-spinel symplectite textures. These intergrowths reflect the breakdown of garnet during decompression into the spinel-peridotite stability field. (e) Plagioclase-type symplectite surrounded by plagioclase-bearing fine-grained mineral aggregate from the Lower Zone lherzolite. Although the grains are so fine that they are difficult to distinguish, plagioclase (Pl) – a low-refractive-index mineral – can be identified surrounding the chromian spinel (S: dark brown fine-grained phase). This texture marks the final stage of the P-T trajectory as the complex transitioned into the plagioclase peridotite stability conditions during its late-stage ascending. Cpx = clinopyroxene, Opx = orthopyroxene, Spl = spinel, Pl = Plagioclase.

Table 1 - Summary of the Horoman peridotites

Peridotite suite	Acronym	Lithology	Sub-types for peridotite in this study	Sub-types for plagioclase peridotite in this study	Note	References
Main Harzburgite Lherzolite Suite	MHL	Plagioclase lherzolite Pyroxene-spinel symplectite lherzolite Spinel lherzolite Spinel harzburgite	Normal-type: The major and trace element compositions exhibit geochemical characteristics consistent with simple residual peridotite following partial melting, and and depleted isotopic signature (high ϵ_{Nd} and low $^{87}Sr/^{86}Sr$) Enriched-type: The major and trace elements DOES NOT exhibit geochemical characteristics consistent with simple residual peridotite following partial melting, and enriched isotopic signature (low ϵ_{Nd} and high $^{87}Sr/^{86}Sr$)	Normal-type Plagioclase peridotite: fertile major element composition (high Al_2O_3 and CaO), and depleted in LREEs, and depleted isotopic signature (high ϵ_{Nd} and low $^{87}Sr/^{86}Sr$) Enriched-type Plagioclase peridotite: refractory major element composition compared to Nromal-Type, cryptic enrichment in incompatible elements and radiogenic isotopes (low ϵ_{Nd} and high $^{87}Sr/^{86}Sr$) Thin layered-type plagioclase peridotite: layering with Type I mafic layers on a millimeter-to-centimeter scale. Clinoppyroxene exhibits high Al and REEs than other plagioclase peridotite types	Dunitic channel with mega-olivine in the MHL harzburgite	Takahashi, 1991, 1992 Takazawa et al., 1992, 2000 Yoshida and Takahashi, 1997 Yoshikawa and Nakamura, 2000 Malaviarachchi et al., 2008, 2010 Ranaweera et al. 2018 Yoshikawa et al., 2019
Spinel-rich Dunite Wehrlite Suite	SDW	Dunite Wehrlite			Only occur within harzburgite of the MHL suite	Takahashi, 1991, 1992 Morishita and Arai, 1997, 2001
Banded- dunite Harzburgite suite	BDH	Dunite Harzburgite Orthopyroxenite			High-Mg, High-Cr Exotic block	Takahashi, 1991, 1992 Matsufuji et al., 2006 Tasaka et al., 2025

Table 2 - Summary of isotopic age dating from the Horoman Peridotite Complex

Lithology	Sample type	Age (Ma)	System	Interpretation	Reference
MHL suite, Normal-type	Whole rock	833 ± 78	Sm-Nd isotope	Melting	Yoshikawa and Nakamura (2000)
MHL suite	Whole rock	910 ± 350	Re-Os isotope	Melting	Saal et al. (2001)
MHL suite, E-type plagioclase peridotite	Whole rock	1860	Re-Os isotope	Re-depletion model age: Older melting?	Saal et al. (2001)
MHL suite, Normal-type plagioclase peridotite	Whole rock	1160 ± 160	Sm-Nd isotope	Melting	Malaviarachchi et al. (2008)
MHL suite, Normal-type plagioclase peridotite	Whole rock + Yoshikawa and Nakamura (2000)	1090 ± 130	Sm-Nd isotope	Melting	Malaviarachchi et al. (2008)
MHL suite, Normal-type plagioclase peridotite	Whole rock	1060 ± 280	Lu-Hf isotope	Melting	Malaviarachchi et al. (2008)
MHL suite, Thin layered-Type mafic layer	Whole rock	257 ± 60	Sm-Nd isotope	Thin layered-type peridotite-mafic layer interaction	Malaviarachchi et al. (2010)
MHL suite, Thin layered-Type mafic layer	Whole rock	313 ± 64	Lu-Hf isotope	Thin layered-type peridotite-mafic layer interaction	Malaviarachchi et al. (2010)
Type I mafic layer	Whole rock	80	Sm-Nd isotope	Formation	Takazawa et al. (1999)
MHL suite + Type I mafic layer	Whole rock	1120 ± 240	Re-Os isotope	Formation	Saal et al. (2001)
Type II mafic layer	Whole rock + Yoshikawa and Nakamura (2000)	830	Sm-Nd isotope	Formation	Takazawa et al. (1999)
Mega olivine-dunite in MHL suite	Clinopyroxene, Olivine and Mega olivine	186 ± 45	Rb-Sr isotope	errochron	Yoshikawa et al. (2018)
Mega olivine-dunite in MHL suite	Clinopyroxene, Orthopyroxene	52 ± 19	Rb-Sr isotope	Crystallization age of pyroxenite veinlet in dunite channel	Yoshikawa et al. (2018)
MHL suite, Phlogopite-bearing	Whole rock & Clinopyroxene	23 ± 1.2	Rb-Sr isotope	Alkali metasomatism	Yoshikawa and Nakamura (1993)
MHL suite, Phlogopite-bearing	Phlogopite	20.6 ± 0.5	^{40}Ar-^{39}Ar	Alkali metasomatism	Kaneoka et al.. (2001)

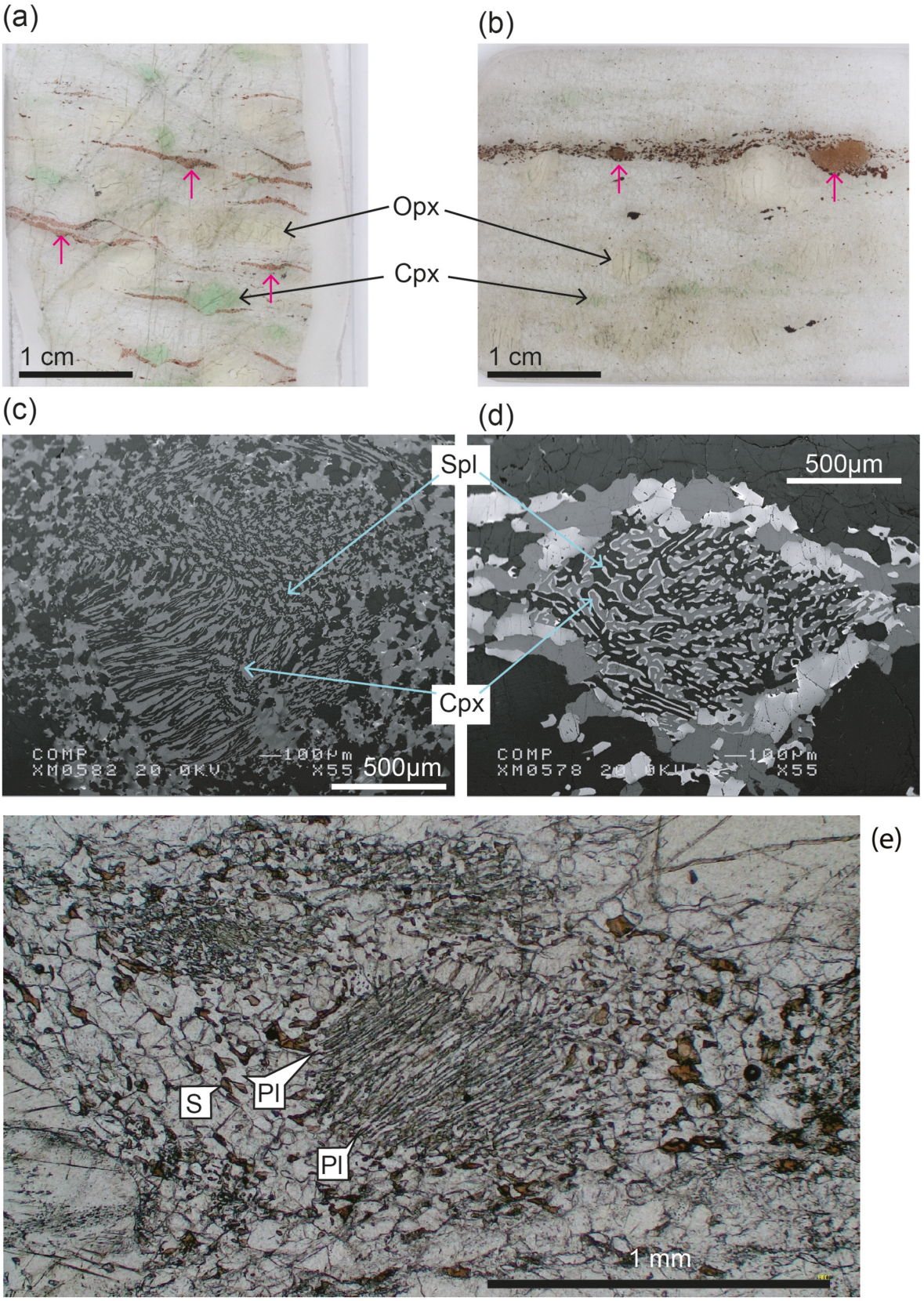

Fig. 5 - Mineral chemical characterization and discrimination of the MHL, SDW and BDH suites. (a) Relationships between forsterite content of olivine (Fo) and the Cr# (Cr/(Cr + Al) atomic ratio) of coarse discrete chromian spinels. The MHL suite reflects a residual mantle origin characterized by variable degrees of depletion in melt components, whereas the SDW suite and the exotic BDH blocks represent distinct petrogenetic processes in the MHL suite. The Olivine-Spinel Mantle Array (OSMA) denotes the compositional range for residual spinel peridotites. (b) Covariation of the forsterite content and NiO wt. % of olivine. The Mantle Olivine Array (OMA) provides a baseline for typical mantle equilibrium compositions. (c) The TiO_2 wt. % versus the Cr# of coarse discrete chromian spinels. Variations in TiO_2 highlight the influence of melt-rock interactions and/or the influence of the intrusion of TiO_2-rich melts that formed the Type I (and Type III) mafic layers. Data in (a) and (b) are simplified and modified after Takahashi (1991). OSMA is from Arai (1994), and OMA is from Takahashi et al., (1987). Compositional ranges for mega olivine-bearing dunite channel (Yoshikawa et al., 2019) are shown by broken line.

The BDH suite is composed of conspicuously layered dunite, harzburgite, and olivine orthopyroxenite, characterized by sharp lithological boundaries. The lithological boundaries between the dunite and pyroxene-rich layers of the BDH suite are parallel to the foliation and lineation of the MHL suite (Takahashi, 1991, 1992; Matsufuji et al., 2006; Tasaka et al., 2025). These layered structures typically exhibit a gentle northward dip, consistent with the broader structural feature of the MHL suite (Matsufuji et al., 2006; Tasaka et al., 2025). Mineralogical characteristics, high Fo olivine and high Cr# spinel (Fig. 5), differ from other two suites. The BDH suite occurs as discontinuous blocks within the MHL suite peridotite (Takahashi, 1991, 1992) (Figs 1 and 2). Matsufuji et al. (2006) suggested that the BDH suite occurs within a limited sequence of the MHL suite in the Upper Zone, which is closely related to the SDW suite. At a specific outcrop (the Nanagome outcrop indicated by the pink arrow in Fig. 1), the BDH suite is in direct contact with the SDW suite (Fig. 4).

Microtexture of olivine (± orthopyroxene)

Although a detailed microtextural analysis falls outside the main scope of this paper, we briefly summarize the primary microtextures of the Horoman peridotites. Niida (1975b) first examined olivine fabric. He analyzed kink bands in coarse-grained olivine and determined that the dominant slip system is (010) axis of olivine in most cases. The preferred lattice orientation of olivine is consistently characterized by a strong concentration of the Z-axis parallel to the lineation throughout the massif. This strong Z-axis maximum is particularly prominent in the Lower Zone. The Upper Zone is distinguished by X-axis maxima concentrated perpendicular to the foliation plane. Sawaguchi and Takagi (1997), Sawaguchi et al. (2001), and Sawaguchi (2004) conducted detailed microstructural analysis based on extensive field work and categorized the Horoman Peridotite Complex into five distinct structural zones aligned with lithological layering following nomenclature of ultramafic rocks of Takahashi (1991, 1992) (as explained later): (1) Equigranular Zone, (2) Internal Shear Zone (ISZ), (3) Transition Zone, (4) Porphyroclastic Zone, and (5) Basal Shear Zone (BSZ) (Fig. 1b), and suggested two primary deformation regimes. The deeper Porphyroclastic and Basal Shear Zones (corresponding to the Lower Zone) exhibit top-to-the-north kinematics, interpreted as the signature of lithospheric extension that facilitated the massif's initial ascent. In contrast, the Equigranular (corresponding to the Upper Zone) and Internal Shear Zones display top-to-the-south shear, consistent with the regional sub-horizontal displacement of the Hidaka lower crustal sequence. The transition to top-to-the-south kinematics was associated with syn-kinematic hydrous mineral growth, such as amphibole, indicating that shear localization continued during retrograde metamorphism. This overprinting was restricted to the Upper Zone, where fluid supply from the surrounding crustal rocks effectively modified the rheological behaviour of the peridotite under wet conditions. The exhumation was completed by further thrusting that brought the complex to the surface within a compressional regime. Matsuyama and Michibayashi (2023, 2024) characterized the spatial heterogeneity of crystallographic preferred orientations (CPOs) of olivine and orthopyroxene in the MHL suite. They reveal a distinct spatial transition of olivine CPOs, migrating from E-type at the structural base (i.e., Lower Zone) to A-, D-, and finally AG-type toward the structural top (i.e., Upper Zone) (Fig. 1b). The basal E-type suggests localized hydrous fluid infiltration during exhumation along major thrusts, whereas the prevalence of AG-type in the upper equigranular units (i.e., Upper Zone) (Fig. 1b) likely reflects syn-kinematic melt involvement or post-deformational annealing. For the latest review on the structural aspects of the Horoman Peridotite Complex, please refer Matsuyama and Michibayashi (2025) and references therein.

Two main mafic layers and unique Type V

The mineral assemblage of "mafic rocks" consists mainly of plagioclase, clinopyroxene, and olivine. Their current mineral assemblages are "gabbroic" (Igi, 1953; Komatsu and Nochi, 1966; Niida, 1974; 1984; Malaviarachchi et al., 2008, 2010), but their texture suggests a metamorphic overprinting rather than igneous origin (Igi, 1953; Takazawa et al., 1999; Morishita et al., 2001). In this manuscript, the mafic rocks of the Horoman Peridotite Complex are referred to as "mafic layer/mafic rock" following Takazawa et al. (1999). Although the current mineral assemblages (plagioclase, clinopyroxene, olivine, etc.) reflect subsolidus reactions, whole-rock compositions allow to discuss their primary mineralogy and genesis.

The mafic layer is classified into several types (up to 5 types), but two types are dominant in the massif (Niida, 1984; Shiotani and Niida, 1997; Takazawa et al., 1999). Two dominant mafic layers are distinguished by mineralogy and chemical compositions (Fig. 8): Type I (Al-Ti augite type), and Type II (Cr-diopside type) mafic layers. Type I and II mafic layers correspond to GBI and GBII of Niida (1984) and Shiotani and Niida (1997), respectively. Type I mafic layers are characterized by higher TiO_2 (> 0.3 wt %) and lower Cr contents, while Type II mafic layers have very low TiO_2 (< 0.1 wt %). It is known that the Type II mafic layer occurs exclusively within the SDW suite (Takazawa et al., 1999; Morishita et al., 2001) (Fig. 2). Interestingly, these two major types of mafic rocks have also been reported from the Ronda (Spain) (Suen and Frey, 1987; Garrido and Bodinier, 1999) and the Beni Bousera (Morocco) (Kornprobst et al., 1990) peridotite massifs.

At the specific outcrop described above where the BDH suite is in direct contact with the SDW suite (the Nanagome outcrop), both Type I and Type III mafic layers are observed at this outcrop (Niida and Takazawa, 2007). The Type III mafic layer exhibits chemical characteristics similar to those of the Type I mafic layer, particularly in terms of their high TiO_2 content within the minerals (Shiotani and Niida, 1997). However, Type III mafic layers have high Cr and Ni contents and are generally thinner than Type I mafic layers (Shiotani and Niita, 1997).

Type V was described by Takazawa et al. (1999). Type V mafic layer represents a subordinate but petrologically distinctive lithology compared to other mafic layers. Type V mafic layer occurs as meter-scale lenticular body hosted in the MHL harzburgite. It consists mainly of orthopyroxene and plagioclase, with minor plagioclase, clinopyroxene and phlogopite. Microtexture of Type V mafic layer is characterized by plagioclase-type symplectite. Whole rock composition of the Type V mafic layer is defined by a highly aluminous yet less silica- and -calcium signature. The trace element patterns of Type V are marked by high HREEs relative to LREEs, depleted in Ti and enriched in Zr and Hf (Fig. 8).

THE FACTORS GOVERNING THE DIVERSITY OF THE HOROMAN PERIDOTITE COMPLEX

Lithological diversity of the Horoman Peridotite Complex records a multi-stage petrogenetic history involving partial melting, melt-rock interaction, metasomatism and metamorphism under dynamic P-T conditions. Here, we first provide a brief introduction of the history of the Horoman Peridotite Complex and briefly discuss some unresolved issues and discrepancies arising from the age data and filed observations (Fig. 9). We introduce, in as chronological an order as possible, the series of events that make the petrological and geochemical diversity of the Horoman Peridotite Complex. Please note that, as mentioned earlier, there is still some debate regarding the timing and interpretations of certain geological events (Fig. 9).

Regarding the origin and history of the Horoman Peridotite Complex, a consensus has been reached on the following two main views: 1) partial melting, melt extraction and crystallization of melt at 1 Ga caused major lithological variation in peridotite (the MHL-SDW suites) and the formation of Type II mafic rock; and 2) the complex ascended from the garnet peridotite stability condition to plagioclase peridotite stability condition. Furthermore, even in the absence of strict age constraints, there is a consensus that late-stage melting, melt-rock interactions and multiple metasomatic processes disrupted the petrological and geochemical characteristics. One of the difficulties in understanding the geochemical diversity of the MHL suite is the influence of cryptic and modal metamorphisms (e.g., Arai and Takahashi, 1989; Takahashi and Arai, 1989; Takazawa et al., 1992, 2000; Yoshikawa and Nakamura, 1993, 2000; Yoshida and Takahashi, 1997; Malaviarachchi et al., 2008, 2010; Ranaweera et al., 2018). Metasomatism is thought to be superimposed by multiple P-T conditions with differing characteristics, both locally and over a wide area. In particular, the temporal and spatial effects of the metasomatic process have not yet been fully elucidated although it has been established that late-stage "alkaline" metamorphism, characterized by the formation of phlogopite and pargasite, occurred at 23 Ma. It is presumed that early-stage metasomatism, i.e., before the ascending of the complex, occurred around 1Ga. Another important factor contributing to the diversity of peridotite is partial melting of plagioclase peridotite and Type I mafic rock as well as their interactions under plagioclase peridotite stability conditions (i.e., this phenomenon implies that it occurred during or after the ascent of the complex) (Ozawa and Takahashi, 1995; Takahashi, 1997, 2001; Yoshida and Takahashi, 1997; Takazawa et al., 2000; Yoshikawa and Nakamura, 2000; Malaviarachchi et al., 2008, 2010; Ranaweera et al., 2018).

Below, we first introduce the earliest melting event at 1 Ga and then introduce the ascending P-T trajectory of the Horoman Complex. The effect of metasomatism and partial melting under plagioclase peridotite stability conditions will be presented later. Several hypotheses have been proposed regarding the origin and evolution of the BDH suite (Takahashi, 1991, 1992; Matsufuji et al., 2006; Akizawa et al., 2021; Tasaka et al., 2025) and the Type I rock (Takazawa et al., 1999; Toramaru et al., 2001; Malaviarachchi et al., 2008, 2010).

The earliest melting events, approximately 1 Ga: the formation of the main lithological variation

The MHL series and the SDW suite (+ Type II mafic layer) constitute the main body of the Horoman Peridotite Complex (Fig. 1). In discussions concerning the petrogenesis of MHL peridotite, the research results of Takahashi (1991, 1992), Takazawa et al. (1992, 1996, 2000), and Yoshikawa and Nakamura (2000) are indispensable.

The relationship between the MHL suite and the SDW suite: the earliest event at c.a. 1 Ga

Before discussing the origin of the MHL suite, it is necessary to highlight the relationship between the MHL suite and the SDW suite. Takahashi (1991, 1992) pointed out that the mineral composition and mineralogy of the MHL rock group are consistent with those of residual peridotite following melt extraction (Takahashi, 1991, 1992). Petrological, mineralogical evidence combined with whole rock composition indicates that the SDW suite is distinct from the MHL suite and is likely to be a cumulate from a magma (Takahashi, 1991, 1992; Yoshida and Takahashi, 1997). One of the most significant findings from the field surveys conducted by Takahashi (1991, 1992) in the Horoman Complex is the limited occurrence of the SDW suite within only harzburgite of the MHL suite (Figs. 1 and 2). These observations indicate that the lithological symmetry of the MHL suite is centered on the SDW suite, and that the basic lithological sequence (Fig. 2) – plagioclase lherzolite -spinel lherzolite-harzburgite-SDW suite-harzburgite-spinel lherzolite-plagioclase lherzolite – is repeated several times within this complex (Fig. 1). It has long been well known that the lithological sequence transitions repeatedly from harzburgite to lherzolite (Niida, 1984), and Obata and Nagahara (1987) proposed a permeability instability model to explain this variation and repetitive pattern in the Horoman Complex. However, since the relationship between SDW and MHL was reported, this model can no longer simply explain the presence of an SDW suite in the central part of the MHL-SDW symmetrical sequence. It is assumed that the basic lithological variations in the MHL and the SDW suites (along with Type II mafic layer, as presented below) were contemporaneously formed during a melting event – the earliest event recorded in the Horoman Complex (approximately 1 Ga). The age data is presented below.

Takahashi (1991, 1992) interpreted that the formation of the SDW suite and the layered MHL suite are attributed to crack formation in upwelling mantle materials. The transport of high-temperature melt of deeper origin caused partial melting along cracks. Partial melts were sucked in and segregated towards these cracks due to local pressure decreasing. Upon cooling, olivine crystallized from the segregated melt on the crack walls, finally forming olivine-clinopyroxene-rich rock, i.e., the SDW suite. However, as will be presented later, the basic lithology of the SDW-MHL suites is thought to have undergone a complex P-T (pressure-temperature) history, likely accompanied by deformation. Therefore, it is highly possible that the original magmatic structure that formed the SDW-MHL suite no longer exists today.

Arai et al. (2021) examined "Black-colored olivine" occasionally found in the SDW dunite, which is caused by a dense distribution of minute, rod-like or dendritic composite inclusions of clinopyroxene and chromian spinel. These dendritic mineral inclusions are interpreted as a reaction of the transition from hydrous to anhydrous olivine where the fayalite and monticellite components of the hydrous olivine react with its internal hydroxyl layers to produce magnetite, diopside, and molecular hydrogen (dehydrogenaition). However, as in this study, dendritic mineral inclusions are commonly found in the mega olivine-bearing dunite in the MHL suite (as presented below). Further research is needed regarding the origin and evolution of the "black-colored olivine" in the Horoman peridotites.

The MHL suite: not simple residue and evidence for the presence of a unique geochemical reservoir

In summary, MHL peridotites exhibit a wide range of chemical variations and can be classified into two types: the "Normal-type", which exhibits geochemical characteristics with simple residual peridotites after partial melting with high $^{143}Nd/^{144}Nd$ (and low $^{87}Sr/^{86}Sr$), and the "Enriched-type", which is characterized by the addition of incompatible elements with low $^{143}Nd/^{144}Nd$ (and high $^{87}Sr/^{86}Sr$) (Figs. 7 and 10) . It is noted that the MHL plagioclase peridotites, particularly in the Upper Zone, are interpreted to record partial melting and melt-rock interaction under the plagioclase stability

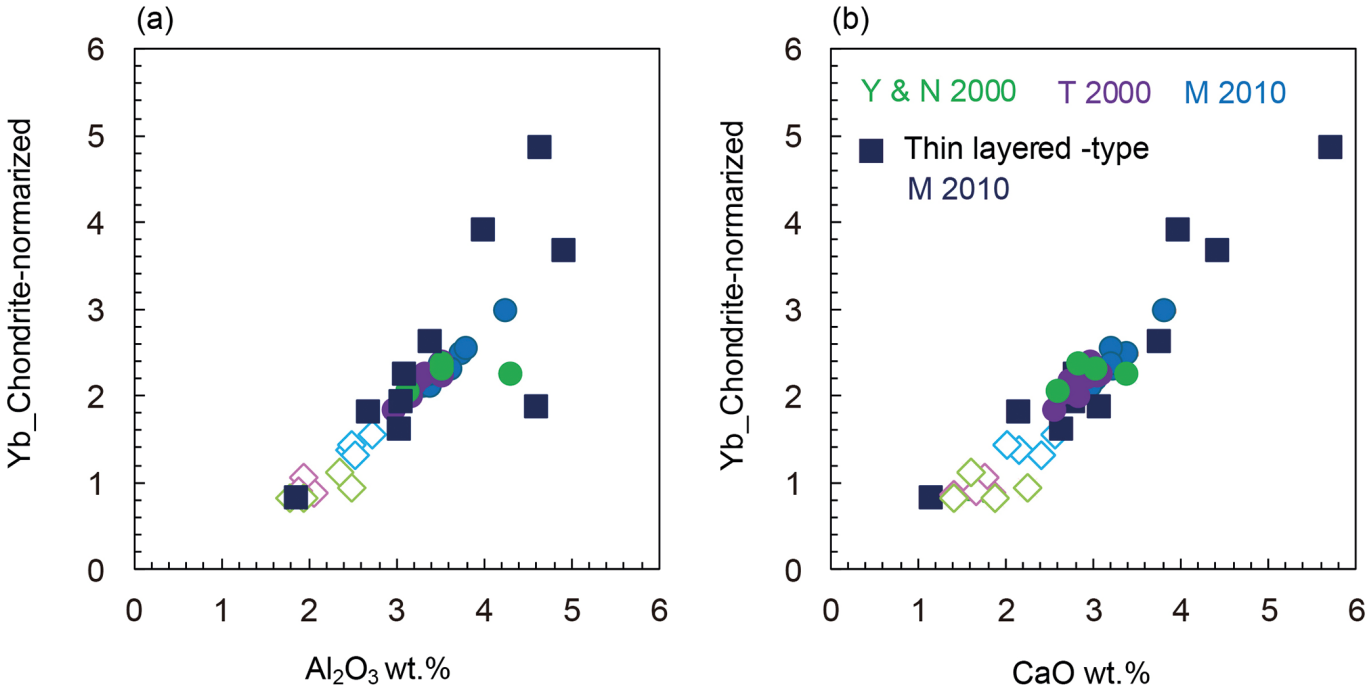

Fig. 6 - Whole-rock major element and heavy rare earth element (Yb) systematics of the MHL plagioclase peridotites. (a) CaO (wt. %) versus chondrite-normalized Yb. (b) Al_2O_3 (wt. %) versus chondrite-normalized Yb value. The observed correlations are consistent with geochemical trends characteristic of a residual mantle origin. Data are compiled from Takazawa et al. (2000) (T 2000), Yoshikawa and Nakamura (2000) (Y & N 2000), and (c) Malaviarachchi et al. (2010) (M 2010). Normalizing values are after McDonough and Sun (1995).

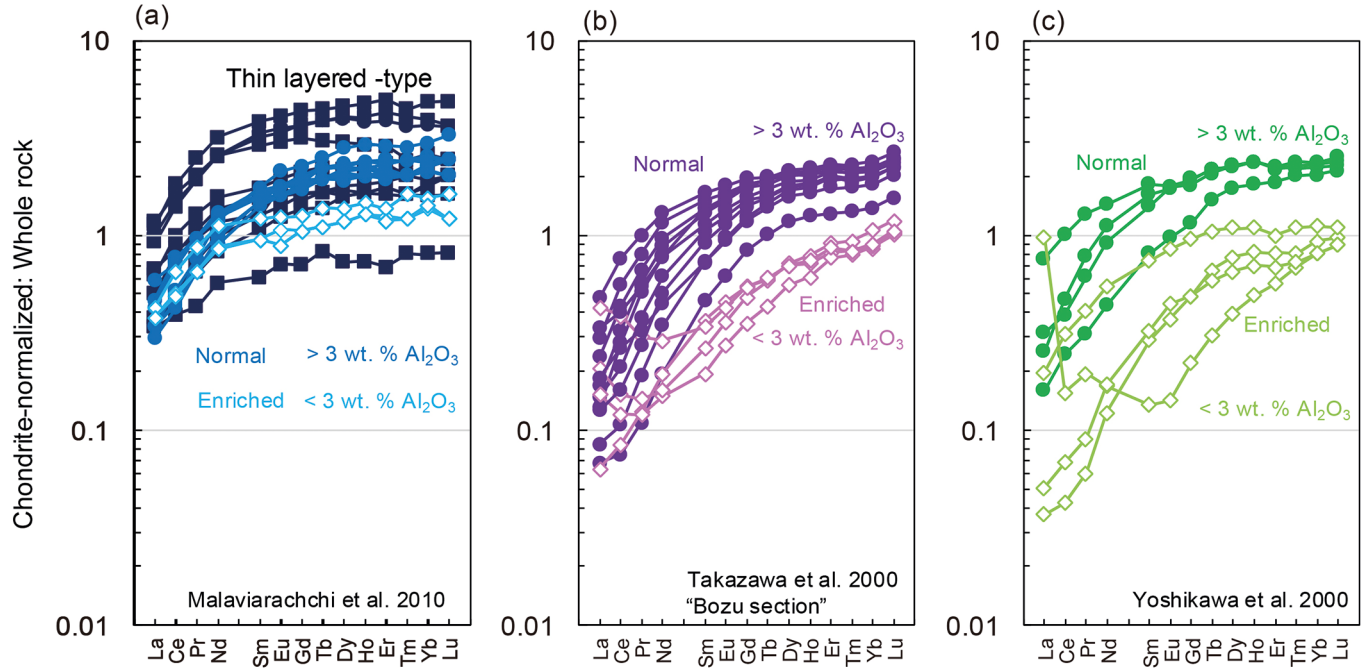

Fig. 7 - Chondrite-normalized rare earth element patterns of whole-rock samples from the MHL plagioclase peridotite. The REE systematics reflect a residual mantle framework formed by the partial melting of a MORB-source (low LREEs/HREEs ratio: Normal-type), overprinted by metasomatism (relatively high LREEs/HREEs ratio: Enriched-type) and late-stage partial melting and melt-rock interaction within the plagioclase peridotite stability conditions (Thin layered-type). See text for more details. To highlight the geochemical transition from Normal-type to more refractory lithologies, samples with Al_2O_3 contents < 3 wt.% are distinguished by open symbols with lighter-colored line. Data are compiled from (a) Malaviarachchi et al. (2008, 2010), (b) Takazawa et al. (2000), and (c) Yoshikawa and Nakamura (2000). Normalizing values are from McDonough and Sun (1995).

field. Although the effects of the low-pressure melting event, i.e., the later melting event, cannot be clearly distinguished from those of the earliest melting event, a distinction between 'Normal' and 'Enrich' types is also recognized in the MHL plagioclase peridotites as described earlier (Takazawa et al., 2000; Yoshikawa and Nakamura, 2000; Ranaweera et al., 2018) (Figs. 6 and 7). Moreover, since the effects of metasomatism will be presented below, here we provide a brief explanation of metasomatism.

Systematic change in mineral chemistry and mineral mode from fertile lherzolite to depleted harzburgite of the MHL suite is consistent with petrological and mineralogical characteristics of residual peridotite after melt extraction (Takahashi, 1991, 1992) (Fig. 5). The HML suite peridotites exhibit extensive whole-rock compositional variations, ranging from fertile lherzolites (~3-4% Al_2O_3 and CaO) to depleted harzburgites (~0.5% Al_2O_3 and CaO), with the fertile end consistent with primitive mantle estimates (Yoshida and Takahashi, 1997; Yoshikawa and Nakamura, 2000; Takazawa et al., 2000, Malaviarachchi et al., 2008, 2010) (Fig. 10). Takazawa et al. (2000) suggested that the systematic variations of whole rock major elements and moderately incompatible elements (such as Na and HREEs) are consistent with a model involving polybaric partial melting model from garnet peridotite stability condition.

While major-element trends in the MHL harzburgite-lherzolite are consistent with residue after varying degrees of partial melting, trace-element and isotopic signatures of whole-rock composition and clinopyroxene require another process, i.e., Enriched-type in this paper (Takazawa et al., 1992, 1996, 2000; Yoshida and Takahashi, 1997; Yoshikawa and Nakamura, 2000) (Figs. 10 and 11). Particularly, Takazawa et al. (1992, 1996, 2000) conducted detailed sampling from a continuous section across a > 100 meter (the Bozu section) from plagioclase lherzolite to harzburgite of the MHL suite including the SDW suite and analyze major and trace element compositions of whole rock and minerals (Fig. 12). Since then, followed by multi-isotope analyses (Saal et al., 2001; Lai et al., 2015; Anguelova et al., 2022) using various analytical techniques on the same sample, support that MHL suite includes peridotites which are not simple residues after partial melting (see Supplementary material).

Takazawa et al. (1992) first reported abrupt shifts in chondrite-normalized REE patterns of clinopyroxene: plagioclase lherzolites exhibit LREE-depleted signatures, whereas samples approaching the harzburgite contact transition into LREE-enriched profiles with distinctive convex-downward slopes, which cannot be reconciled with simple residue models (Fig. 13). Yoshida and Takahashi (1997) measured trace element compositions across the complexes and suggested that spinel lherzolites and harzburgites of the MHL suite show enrichments in Sr and Ti relative to Zr and Y. These patterns support a cryptic metasomatic overprint through the addition of a melt component to the pre-existing heterogeneous mantle

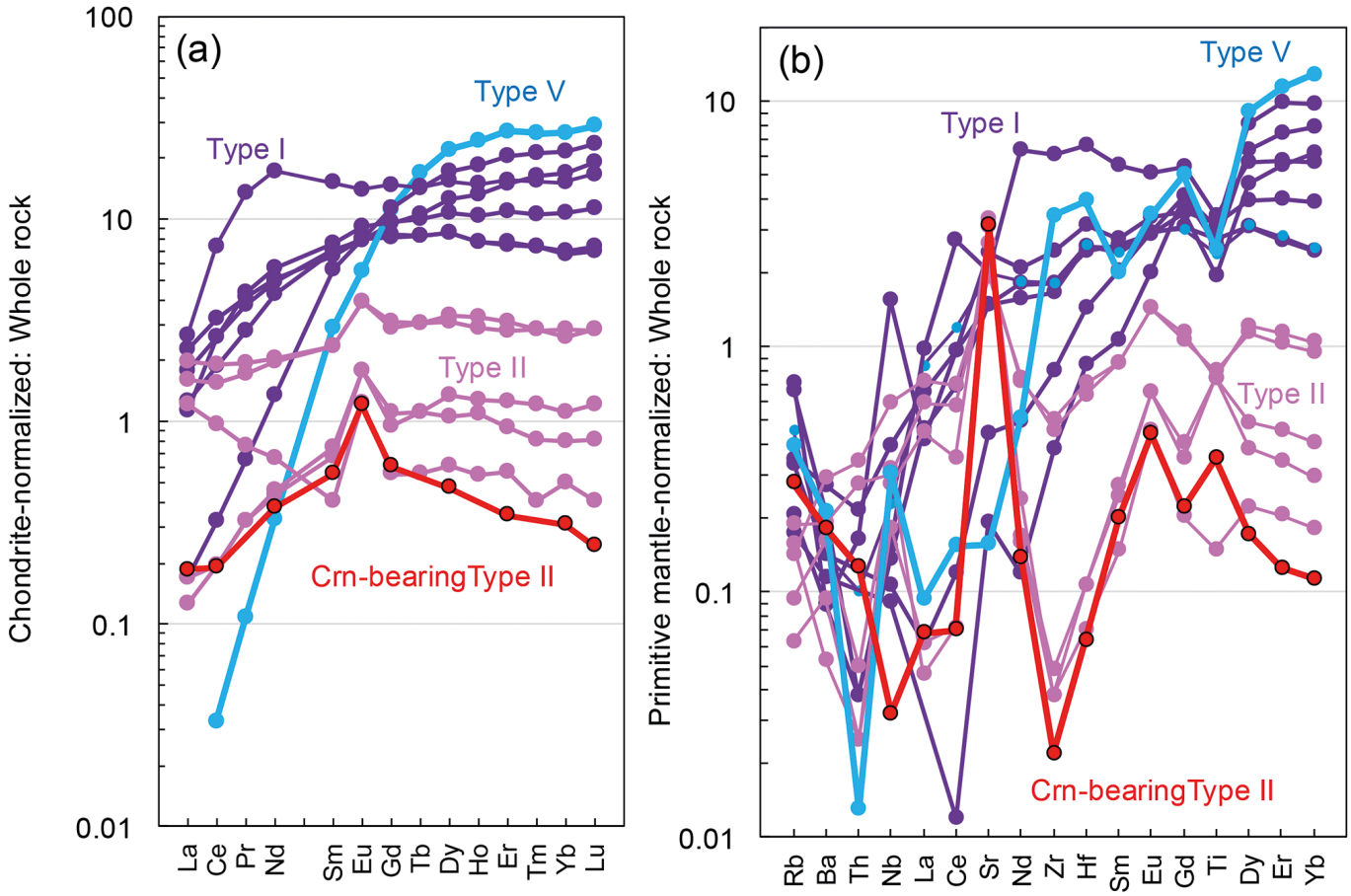

Fig. 8 - Geochemical characteristics of mafic layers of the Horoman Peridotite Complex. (a) Chondrite-normalized rare earth element patterns and (b) extended trace element patterns of whole-rock samples from Type I, Type II, and Type V mafic layers. The diverse geochemical signatures reflect a complex petrogenetic history involving igneous protolith formation, high-pressure metamorphism, and subsequent metasomatism. Chondrite normalizing values are from McDonough and Sun (1995). Data sources: Takazawa et al. (2000) and Morishita et al. (2004).

section, probably formed by the earliest magmatic event. Takazawa et al. (2000) further analyzed whole rock major and trace element composition of the Bozu section samples and reported two distinct plagioclase peridotites (Fig. 12): the Normal-type plagioclase lherzolite represents the most fertile lithology within the massif, characterized by high whole rock concentrations of basaltic components with REE profiles showing smooth depletion from middle to LREEs, and the Enriched-type plagioclase lherzolite being significantly more depleted in basaltic components with "enriched" REE patterns (high La/Sm ratio) (Figs. 9 and 10).

Rehkamper et al. (1999) reported clear correlations between PGE ratios (Pt/Ir and Pd/Ir) and lithophile element concentrations (Al_2O_3, CaO) for the MHL peridotites from

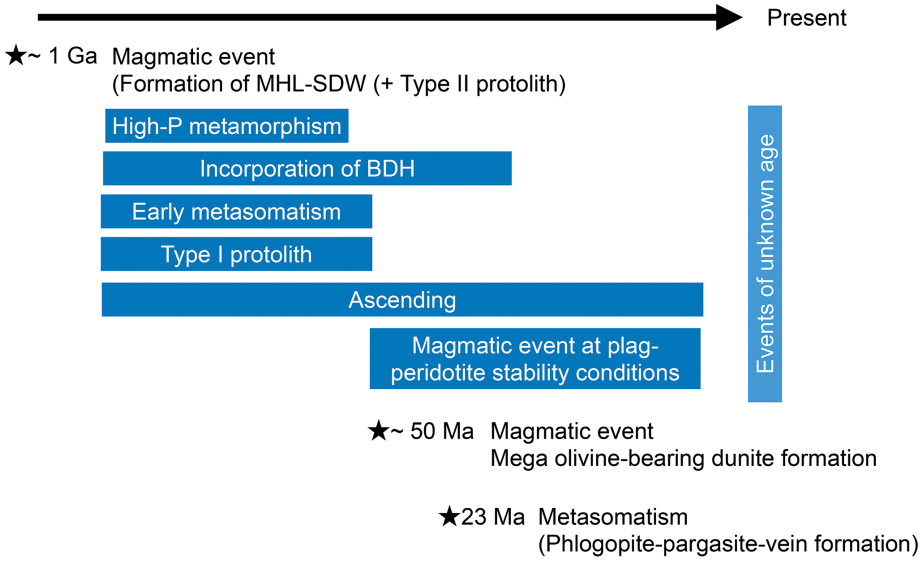

Fig. 9 - A brief overview of the factors contributing to the diversity of the Horoman Peridotite Complex. The text in white on a blue background refers to an age unknown event.

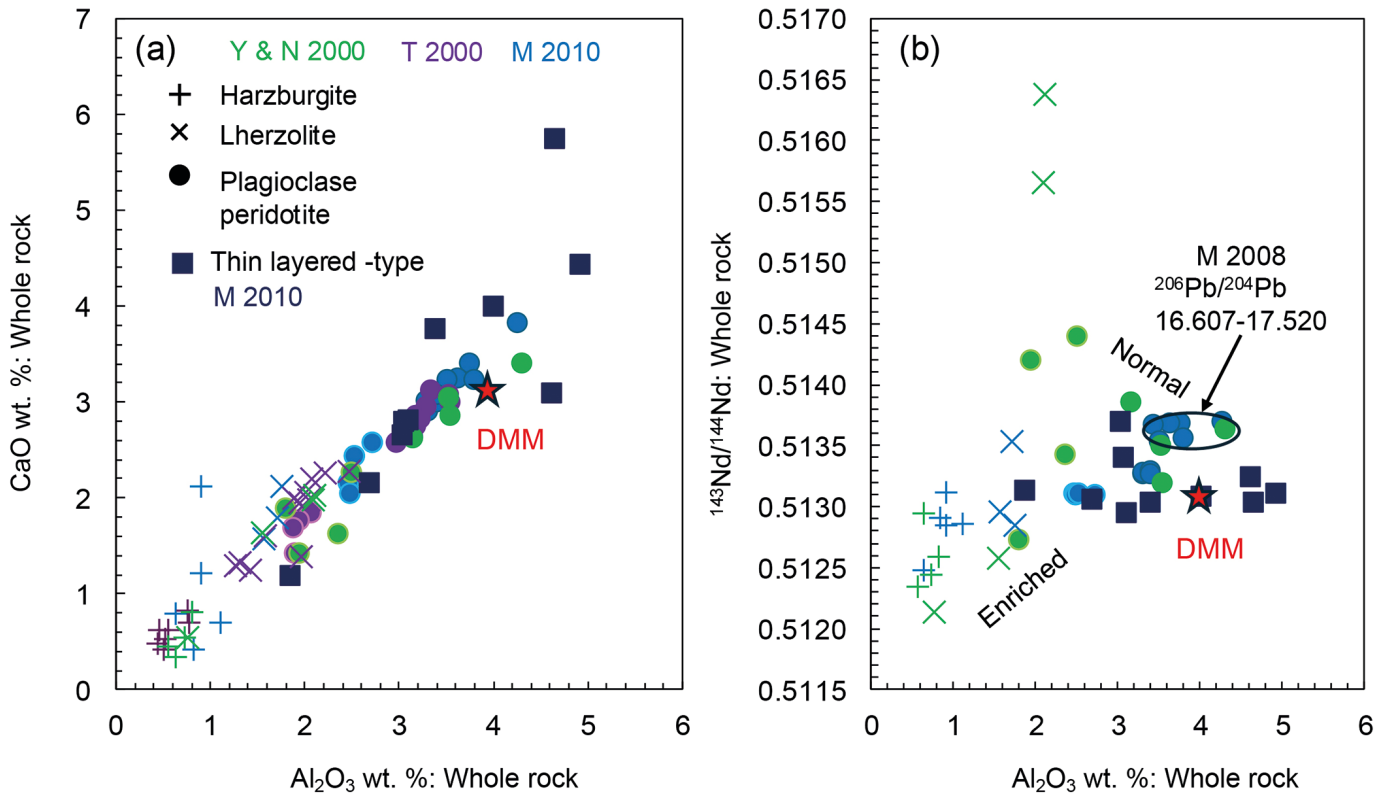

Fig. 10 - Whole-rock major element and isotopic systematics of the MHL peridotites. (a) CaO versus Al_2O_3 (wt. %). The strong linear correlation illustrates the variable degrees of depletion in the MHL suite, which originated as a residual mantle following the partial melting of a MORB source mantle. (b) Al_2O_3 wt. % versus $^{143}Nd/^{144}Nd$ isotopic ratios, showing samples characterized by unradiogenic Pb signatures. These variations demonstrate two geochemical trends indicating depleted mantle (high Nd-isotope: Normal-type) and residual peridotite overprinted by subsequent melt-rock interactions and multi-stage metasomatism (low Nd-isotope: Enriched-type). The composition of the Depleted MORB Mantle (DMM) is from Workman and Hart (2005) for reference.

the Bozu section, such that the most fertile lherzolites are characterized by non-primitive (high) PGE ratios. Simple melt extraction alone cannot explain the high Pd/Ir ratios of the MHL lherzolites. The observed geochemical systematics require more complex processes, likely involving melt depletion followed by re-enrichment in sulfides derived from percolating magmas, potentially combined with the addition of a basaltic melt component (i.e., refertilization). The high Pd/Ir and Pt/Ir ratios in the Bozu lherzolites are likely generated both by the addition of Pd and Pt through sulfides and by secondary depletion of Ir and Ru via processes such as the progressive dissolution of trace carrier phases (e.g., alloys) in percolating magmas. Interestingly, microbeam synchrotron X-ray fluorescence analysis of MHL lherzolite samples identified trace amounts of platinum group minerals (PGMs) (Koghiso et al., 2008), suggesting that these might be the primary cause of the nugget effect observed in whole-rock PGE analyses (Koghiso et al., 2008). Furthermore, Kitakaze et al. (1998, 2008, 2011) reported Cu-Fe-Ni sulfide minerals, including new discoveries from the Horoman Peridotite Complex, which are closely associated with native copper. Ikehata and Hirata (2012) performed copper isotope analyses on native copper grains and the corresponding whole rock sample (MHL plagioclase lherzolite). These results are shown in the supplementary file.

Age constraints related to the earliest melting event

Here, we introduce the age data most likely associated with the earliest melting events. Yoshikawa and Nakaura (2000) reported that the MHL peridotite can be classified into two types: Depleted Peridotite (DP) (Normal-type in this paper), which retain LREE and LIL element depletion characteristic of melt extraction residues from a MORB mantle source (similar to N-Type of Takazawa et al., 2000), and Enriched Peridotite (EP) samples (Enriched-type in this paper), which exhibit enriched LREE, Sr, Ba, and Pb signatures indicative of metasomatism (similar to E-type of Takazawa et al., 2000) (Figs. 7 and 8). Yoshikawa and Nakamura (2000) suggested that the MHL peridotites exhibit extremely large variations in Sr and Nd isotopic compositions ($^{143}Nd/^{144}Nd$ from 0.5164 to 0.5121 (Fig. 10); $^{87}Sr/^{86}Sr$ from 0.7019 to 0.7066), confirming the influence of both melt depletion and enrichment (Fig. 7). The Nd isotopic data for the Normal-Type peridotites suggest the initial melt extraction event occurred at 833±78 Ma, corresponding to an initial $^{143}Nd/^{144}Nd$ ratio of 0.5119±2, consistent with extraction from a MORB source. Saal et al. (2001) measured Re-Os isotopic data for the Bozu peridotites and two Type I mafic layers. These samples exhibit a range in $^{187}Os/^{188}Os$ ratios from 0.1158 to 0.1283. Strong positive correlations are observed between $^{187}Os/^{188}Os$ ratios, Re content, and the abundances of basaltic components, such as Al_2O_3, Sc, Yb, and modal clinopyroxene. The Re-Os data define an apparent age of 910 ± 350 Ma for MHL peridotites excluding Enriched-type plagioclase peridotite. Conversely, the lowest $^{187}Os/^{188}Os$ ratio (0.1158) in an Enriched-type plagioclase lherzolite yields a minimum Re depletion model age of > 1860 Ma, suggesting an older depletion event.

Malaviarachchi et al. (2008, 2010) classified the MHL peridotites and mafic layers into two major types by their spatial scale and field relationships: the thin-layer type peridotite and gabbro (note they refer to mafic layer as gabbro) (TLP and TLG) and the massive type peridotite and gabbro (MSP and MSG). Massive Plagioclase Lherzolites are interpreted as unmetasomatized partial melting residues, exhibiting LREEs-depleted patterns (i.e., Normal-type) (Figs. 6 and 7). In contrast to the Normal-type (Massive Plagioclase Lherzolites), the more refractory spinel lherzolites and harzburgites show evidence of extensive metasomatic overprinting, which is characterized by the LREE enrichment (Fig. 10) and elevated concentrations of fluid-mobile elements (e.g., Ba, Rb,

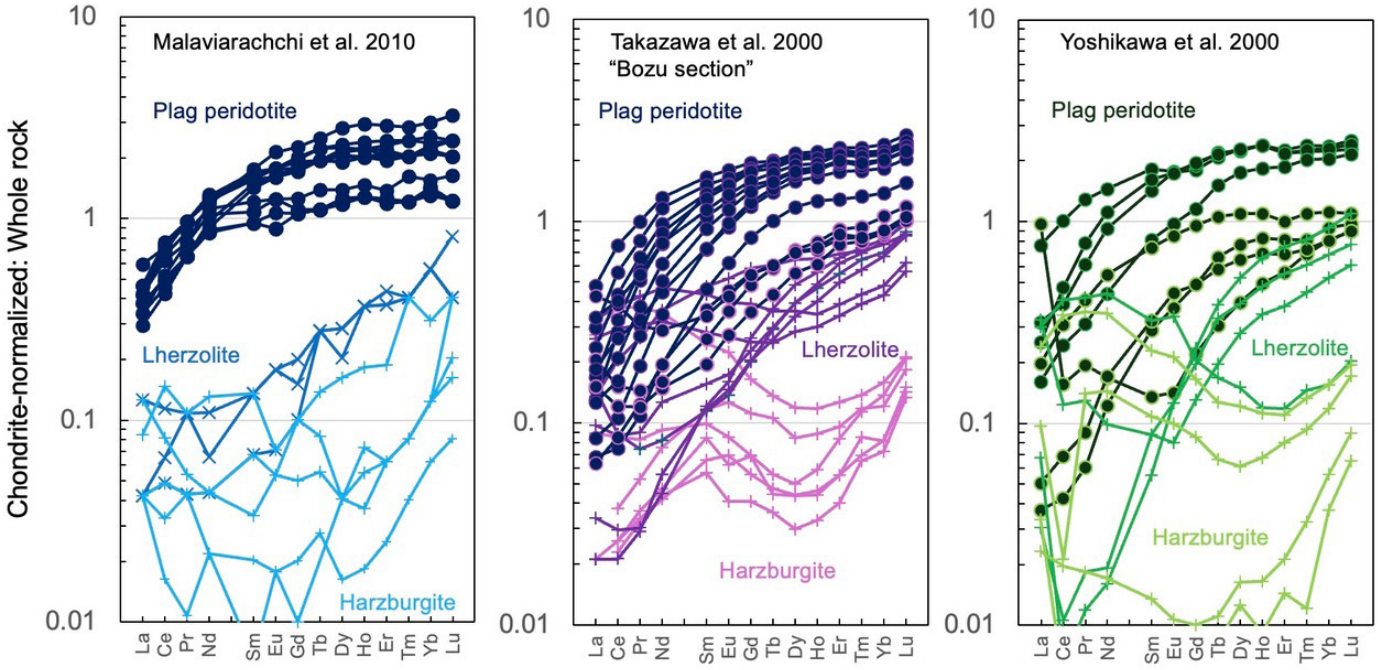

Fig. 11 - Chondrite-normalized rare earth element (REE) patterns of whole-rock samples from the MHL peridotites. The geochemical signatures represent a residual mantle formed through partial melting of a MORB source mantle, exhibiting variable degrees of depletion (low LREEs/HREEs ratio: Normal-type). These patterns also reflect the overprinting effects of multi-stage metasomatism and melt-rock interactions (relatively high LREEs/HREEs ratio: Enriched-type). Chondrite normalizing values are from McDonough and Sun (1995). Data are compiled from Takazawa et al. (2000), Yoshikawa and Nakamura (2000), and Malaviarachchi et al. (2008, 2010).

Cs, and Pb) (i.e., Enriched-type). Isotopic analysis of the Normal-type (Massive Plagioclase Lherzolites), yields isochron ages of an approximately 1 Ga (Malaviarachchi et al., 2008): the Sm-Nd system defines an age of 1.16 ± 0.16 Ga, while the Lu-Hf system provides a concordant age of 1.06 ± 0.28Ga. When these data are integrated with previous Sm-Nd studies of Yoshikawa and Nakamura (2000), they converge on an age of 1.09 ± 0.13 Ga. Akizawa et al. (2021) carefully examined the age data published from the MHL suite and suggested that the age of 833 ± 78 Ma is reliable due to the use of a spatially continuous set of samples with a wide range of Sm/Nd ratios.

In summary, the main melting stage of the Horoman Peridotite Complex, dated to approximately 1 Ga, involved the decompression-induced partial melting of a MORB-source mantle during its ascent across the garnet-spinel transition. This primary melting event generated the spectrum of depletion signatures preserved in the MHL residual suite and was contemporaneous with the development of the SDW suite within the shallow oceanic lithosphere. This foundational depletion signature was subsequently modified by melt-rock interactions and multi-stage metasomatic overprinting, which modified the residual geochemical characteristics.

Early metasomatism and the origin of metasomatic agents

The metasomatism, which is defined here as changes in geochemical composition and mineral modes, is attributed to multiple infiltrations of fluids and/or melts, including melts derived from the partial melting of ultramafic-mafic lithologies within plagioclase peridotite stability conditions. Here, metasomatism in the Horoman complex is categorized into three aspects:

1. Early cryptic metasomatism, identified through specific geochemical signatures.
2. Reactive interactions between host peridotite and either the melts responsible for mafic layer formation or partial melts derived from lherzolite and existing mafic layers under plagioclase peridotite stability conditions.
3. Late-stage "alkaline" metasomatism at 23 Ma, characterized by the formation of phlogopite and pargasite.

While deciphering the specific genetic links between distinct metasomatic signatures and individual overprinting events remains challenging, the alkaline metasomatism is clearly identified as a late-stage process, as separately presented below. A significant ambiguity persists regarding the extent to which broader metasomatic characteristics are genetically related to this "alkaline metasomatism" event. Despite these uncertainties, we present several critical results that elucidate the early metasomatic evolution of the Horoman Peridotite Complex. The effects of melting and its interactions under plagioclase peridotite stability conditions will be also presented later.

Trace element compositions of clinopyroxene and whole rock in the Enriched-type MHL peridotites reveal evidence that harzburgites and lherzolites reacted with an exotic fluid or melt (Fig. 13). Takazawa et al. (1992) explained that these geochemically enriched features are the products of chromatographic fractionation during the percolation of an exotic, LREE-rich melt through a peridotite matrix, based on numerical simulations using a 1-D porous flow model. Takazawa et al. (1996) suggested that this metasomatic (enrichment) process preceded the sub-solidus breakdown of garnet and the subsequent decompression history recorded in the pyroxene zoning.

Takazawa et al. (2000) also pointed out abrupt compositional and modal changes at lithological boundaries (Fig. 12). They suggested that possible origins for abrupt changes in lithology and geochemistry are related to permeability instability (Obata and Nagahara, 1986) coupled with mineralogical variation in the partially molten peridotite (Toramaru and Fujii, 1986), phase saturation boundaries during melt-rock reaction, or mechanical juxtaposition of residues formed at different melting extents. Subsequent stretching and bending within the lithospheric mantle might have transformed a simple structure into the observed cyclic layered sequence (Toramaru et al., 2001). The pronounced compositional heterogeneity observed on the meter scale in the Bozu section (Takazawa et al., 1992, 2000; Rehkamper et al., 1999), including the juxtaposition of Normal -type plagioclase peridotites with suprachondritic $^{187}Re/^{188}Os$ ratios and Enriched-type plagioclase peridotites with anomalously low $^{187}Os/^{188}Os$ ratios just 5 m apart, is also confirmed.

Obata and Takazawa (2004) proposed a physical model in which melt segregation is an episodic process triggered by the topological transformation of melt geometries within a gravitational field, involving a critical transition in microstructure of melts from interconnected channel to isolated pockets forming an impermeable barrier responding to the balance between local fluid pressure and solid pressure. Decompression melting eventually leads to a critical fraction of melt, triggering a rapid microstructural reorganization that abruptly restores permeability of the host rock and the ability of the melt to percolate. This permeability front migrates through the melting matrix, releasing accumulated melt as discrete melt batch. They suggested that this model accounts for the sharp depletion fronts observed in the Bozu section. However, this model fails to explain the presence of the SDW suite within harzburgite, which has a lower melt fraction among the MHL suite in their model.

Based on integration of trace element systematics, particularly high B/Nb and Pb/Ce ratios, Yoshikawa and Nakamura (2000) suggested the metasomatic agent as an aqueous fluid derived from a subducting slab in being equilibrated with crustal or sedimentary components rather than silicate melts.

Helium and argon isotopic analyses on MHL suite revealed that these samples contain a complex noble gas signature exhibiting both mantle and atmospheric components. The samples display uniform $^{3}He/^{4}He$ ratios (7.7-9.2 *Ra*) and $^{4}He/^{40}Ar$ ratios (1.5-3.4), values consistent with those suggested for the MORB source (Matsumoto et al., 2001; Kobayashi et al., 2018). In contrast, the measured $^{40}Ar/^{36}Ar$ ratios (330-470) are low compared to typical MORB source values (~40,000) (Ikeda et al., 2001). This low ratio indicates a substantial contribution from an atmospheric component, suggesting that virtually all ^{36}Ar resides in the samples is of atmospheric origin.

Halogen (I/Cl and Br/Cl) compositions obtained from fluids released by stepped crushing from the MHL peridotites are similar to those found in marine sedimentary pore fluids and serpentinites (Kobayashi et al., 2017). While the halogen signature aligns closely with sedimentary pore fluid, the MHL peridotite exhibits noble gas elemental ratios, specifically slightly higher $^{84}Kr/^{36}Ar$ and $^{132}Xe/^{36}Ar$ ratios compared to seawater. This deviation from a simple mixing line of seawater and unfractionated air is not attributed to altered oceanic crust, but instead suggests that the initial seawater-like noble gas elemental ratios likely underwent fractionation during complex processes such as partial melting and crystallization (Kobayashi et al., 2017).

Collectively, the trace element and isotopic signatures of the enriched peridotites and mafic layers point to a sub-

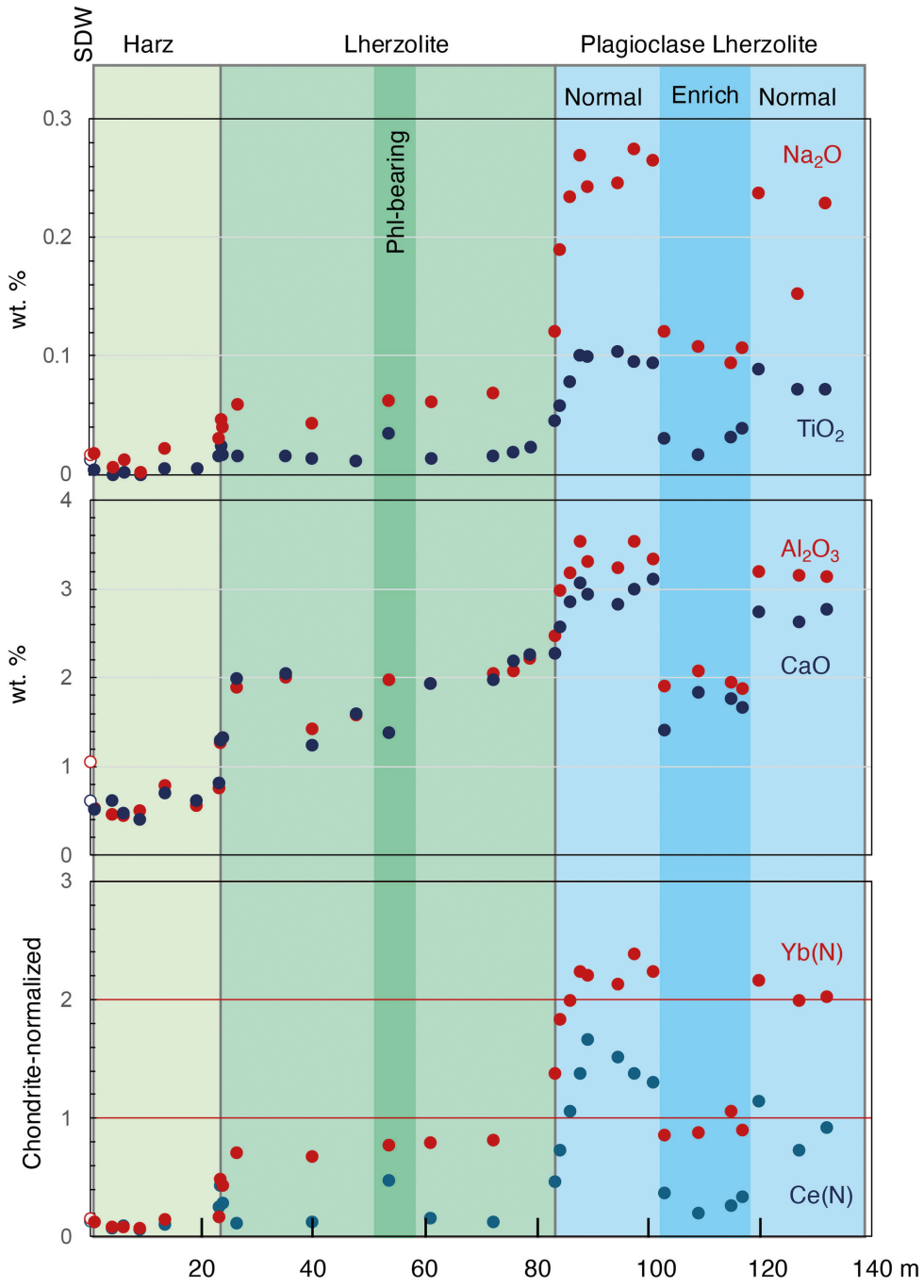

Fig. 12 - Whole-rock geochemical profiles of MHL peridotites across the Bozu section of the Horoman Peridotite Complex. The data illustrate abrupt geochemical discontinuities in chemical abundances across major lithological boundaries within the MHL suite. The profiles highlight the occurrence of "Enriched-type" (Enrich) plagioclase peridotite within "Normal-type" (Normal) plagioclase lherzolite sequence. These variations are interpreted as the result of localized refertilization, probably caused by melt-rock interaction. The presence of phlogopite marks the influence of alkali metasomatism, which occurred at approximately 23 Ma and locally modified the whole-rock compositions. Data are from Takazawa et al. (2000). Chondrite normalizing values are from McDonough and Sun (1995). SDW = Spinel-rich Dunite-Wehrlite suite, Harz = harzburgite, Phl = phlogopite, Normal = Normal-type plagioclase peridotite, Enrich = Enriched-type plagioclase peridotite.

ducted slab origin for the metasomatic agent, indicating that all lithologies within the Horoman Peridotite Complex were metasomatized, within the mantle wedge or via interaction with the surrounding metamorphic rocks during exhumation, or both.

Type II mafic layer: Evidence supporting the earliest melting events, as well as indications of changes in P-T conditions preceding the ascending of the complex

Type II mafic layers are chemically characterized by lower incompatible element abundances and relative enrichments in Sr and Eu, being consistent with the important proportion (> 50%) of cumulus plagioclase (Fig. 8). These layers are interpreted to have formed as plagioclase-rich cumulates within the plagioclase stability field (Takazawa et al., 1999; Morishita et al., 2004; Malaviarachchi et al., 2010). However, symplectitic mineral aggregate also occurs in clinopyroxene-rich layers within the SDW suite and the Type II mafic layer of the Lower Zone, suggesting that both SDW and the Type II mafic layer are likely derived from the garnet peridotite stability conditions (Morishita and Arai, 1997). These differences in the P-T conditions of this Type II mafic layer were elucidated by the discovery of a Type II mafic layer containing corundum (Morishita and Kodera, 1997; Morishita and Arai, 2001; Morishita et al., 2004). Whole-rock trace-element signatures of these rocks are like oceanic gabbros or troctolites. Plagioclase-rich gabbro, which is abundant in Al_2O_3, can be explained as a protolith for the corundum-bearing Type II mafic layer. Piston-cylinder experiments on aluminous mafic compositions identical to the corundum-bearing Type II mafic rock suggest that corundum is stable between 2.0 and 3.0 GPa, corresponding to garnet peridotite stability conditions. This result combined with whole rock compositions

of the Type II mafic layers indicates that the low-pressure cumulate protoliths were subsequently metamorphosed at the upper mantle conditions without undergoing significant partial melting (Morishita et al., 2004).

The Nd isotopic systematics of Type II layers are consistent with the 831 Ma whole-rock peridotite isochron defined by the host MHL peridotites (Takazawa et al., 1999). The initial $^{143}Nd/^{144}Nd$ ratio, as defined by the isochron, corresponds to the MORB mantle at that time (Takazawa et al., 1999). It should be emphasized that the Type II mafic layer occurs exclusively within the SDW suite (Takazawa et al., 1999; Morishita et al., 2001). These data support that Type II layers formed at the same time of the host MHL peridotite and experienced the earliest partial melting, followed by high-pressure metamorphism.

Type I mafic layer: Its origins and history are not yet fully understood

Thick layer of the Type I mafic layer exhibits significant intralayer compositional heterogeneity (Takazawa et al., 1999). The centers of thick layer have lower Mg-number (100 $Mg/(Mg + Fe^{total})$ ratio), lower abundances of highly incompatible elements, and higher abundances of HREEs compared to their margins. Takazawa et al. (1999) suggested that the centers are interpreted as garnet clinopyroxenite cumulates, i.e., high-pressure cumulate, whereas the margins are inferred to represent the melt that was in equilibrium with these cumulates. Isotopic data indicate that Type I mafic layers formed from MORB-related melts (Takazawa et al., 1999; Malaviarachchi et al., 2010). Two-point Nd isotope isochrons for the centers and margins of the thick layers yield a formation age of approximately ~80 Ma (Takazawa et al., 1999).

On the other hand, Saal et al. (2001) measured Re-Os isotopic data for two Type I mafic layers. These samples exhibit a range in $^{187}Os/^{188}Os$ ratios from 0.1158 to 0.1283. Strong positive correlations are observed between $^{187}Os/^{188}Os$ ratios, Re content, and the abundances of basaltic components, such as Al_2O_3, Sc, Yb, and modal clinopyroxene. The Re-Os data define an apparent age of 910 ± 350 Ma for MHL peridotites excluding Enriched-type plagioclase peridotite (see below for Enriched-type plagioclase peridotite). Including the Type I mafic layers with the MHL peridotites from the Bozu section in the regression yields an apparent age of 1120 ± 240 Ma. Although these trends are not true isochrons, Saal et al. (2001) suggested that the consistency of the > 900 Ma age with the 833 ± 78 Ma age derived from Sm-Nd isotopes (Yoshikawa and Nakamura, 2000) indicates this age has geological significance, a genetic relationship between the Type I mafic layer and ultramafic rocks.

It should be emphasized that the implications of the age data for Type I mafic layers remain unclear, as the mafic layers and plagioclase peridotites in the Upper Zone are expected to be affected by partial melting and interactions with surrounding rocks within the plagioclase peridotite stability conditions as introduced later.

Ascent of the Horoman peridotite Complex

The origin of symplectite: garnet breakdown

The formation of pyroxene-spinel symplectite is interpreted as a subsolidus decompression reaction product between garnet and olivine that occurred during the ascent of the Horoman Peridotite complex, indicating its derivation from garnet peridotite stability condition (Kushiro and Yoder, 1966; Tazaki et al., 1972; Takahashi and Arai, 1989; Ozawa and Takahashi, 1995; Takazawa et al., 1996; Morishita and Arai, 2003). The estimated bulk chemical composition of pyroxene-spinel symplectite in the Lower Zone lies within the mixed compositional range of pyrope-rich garnet and olivine for both major and trace elements (Takahashi and Arai, 1989; Morishita & Arai, 1997, 2003, Obata et al., 1997). The trace element compositional zoning observed in clinopyroxene porphyroclast in the MHL lherzolite reflects a subsolidus transition during the exhumation process from garnet lherzolite stability condition (Takazawa et al., 1996, Yoshikawa and Nakamura, 2000; Morishita and Arai, 2003). While the core of clinopyroxene porphyroclast retains a composition equilibrated with garnet, the porphyroclast rim and clinopyroxene neoblast reflect subsequent re-equilibration under low-pressure conditions for spinel-to-plagioclase peridotite stability condition. (Figs. 13c and 13d).

Differences in P-T trajectory between the Upper and Lower Zones inferred from the chemical zoning of minerals

Ozawa and Takahashi (1995) estimated the decompression path of the MHL peridotites by combining the chemical zoning patterns of pyroxene and plagioclase with a numerical diffusion model. The pressure-temperature (P-T) trajectory estimated by Ozawa and Takahashi (1995) is revised based on a detailed chemical analysis of centimeter-sized orthopyroxene and clinopyroxene grains (megacrysts) found in the Upper Zone (Ozawa, 1997, 2004) (Fig. 14). These megacrysts provide critical information regarding the P-T conditions of the garnet peridotite stability field, which were previously ambiguous using smaller porphyroclastic grains ($\lesssim$5 mm). The cores of the Upper Zone pyroxene megacrysts show significantly lower aluminum (Al) and calcium (Ca) contents than the cores of the smaller pyroxene porphyroclasts previously studied in the Upper Zone. Applying geothermobarometry, to the stable core compositions of the large megacrysts yields much better constrained initial P-T estimates for the pre-ascent conditions. The Upper Zone equilibrated at 1070 ± 30°C and 2.3 ± 0.11 GPa, conditions substantially hotter and deeper than the Lower Zone, which equilibrated at 950 ± 20°C and 1.9 ± 0.07 GPa (Ozawa and Takahashi, 1995). In contrast, the increase of Al content from the core toward the margin in Lower Zone porpyroclast pyroxenes suggests nearly adiabatic decompression from the initial conditions of the garnet peridotite stability field into the spinel peridotite stability conditions (Ozawa and Tahakashi, 1995). Subsequent decompression is documented by plagioclase zoning in fine-grained aggregates, indicating continuous upwelling from the spinel peridotite stability field into the plagioclase peridotite stability field. Plagioclases show a decrease in the Na-Ca ratio (increase in anorthite content) from core to rim. This plagioclase zoning, along with the sharp decrease in Al and Ca toward the pyroxene rims, suggests the occurrence of fairly rapid cooling associated with continuous decompression during the final ascent of the complex. The minimum P-T condition from the pyroxene rims is estimated at approximately 750–850 °C and 0.5 GPa across both Upper and Lower Zones (Ozawa and Takahashi, 1995).

Another important revision by Ozawa (1997, 2004) involves the identification of a thermal heating event that strongly influenced the Upper Zone (UZ) ascent trajectory (Fig. 14). Mineral chemistry recorded in the marginal zones of the UZ orthopyroxene megacrysts points to a significant thermal perturbation. The maximum Ca content in the

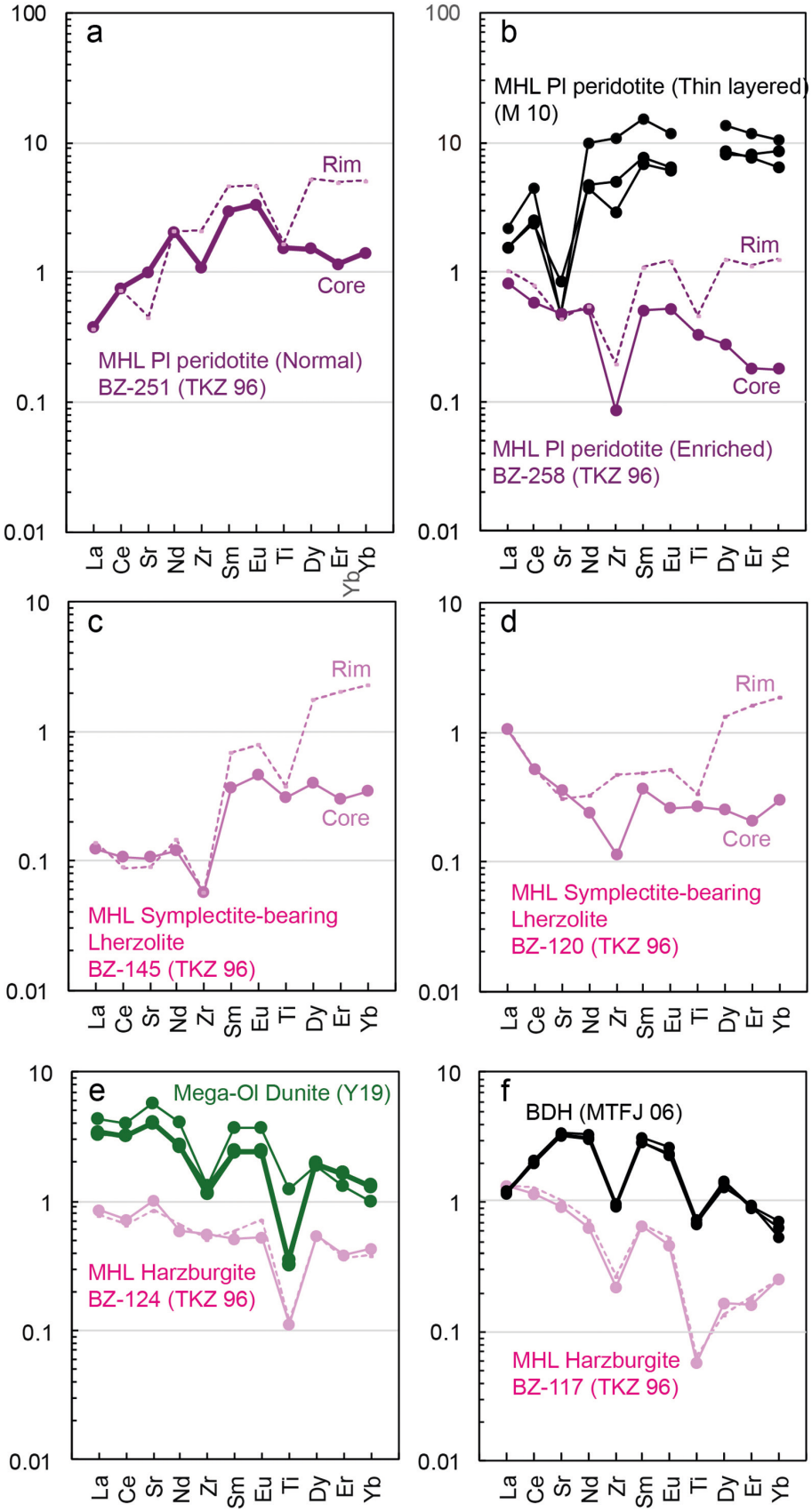

Fig. 13 - Primitive mantle-normalized trace element patterns of representative clinopyroxene of the MHL suite, mega olivine-bearing dunite, and the cpx-bearing BDH suite. (a), (b) MHL plagioclase peridotite (Pl peridotite). (c), (d) MHL symplectite-bearing lherzolite. The core retains a composition equilibrated with garnet, whereas the rim reflects subsequent re-equilibration under low-pressure spinel-peridotite stability conditions (Takazawa et al., 1996). (e) MHL harzburgite and mega olivine-bearing dunite. (f) MHL harzburgite and cpx-bearing BDH. Primitive mantle values are from McDonough and Sun (1995). Data are from Takazawa (1996) (TKZ 96), Malaviarachchi et al. (2010) (M 10), Yoshikawa et al. (2019) (Y19), and Matsufuji et al. (2006) (MTFJ 06).

marginal zones of orthopyroxene megacrysts corresponds to peak temperatures as high as 1200 °C at approximately 1.0 GPa. This indicates that the Upper Zone experienced a temperature rise of about 130 °C while passing through the spinel stability field.

Based on the revised P-T trajectory combined with structural data, Ozawa (2004) suggested that the Horoman Peridotite Complex underwent substantial tectonic thinning driven by the diapiric ascent of hot asthenospheric mantle into the lithosphere. The observed stratification where the initially deeper (hotter) Upper Zone now overlies the Lower Zone is interpreted as a result of the overturning of the lithospheric section (Ozawa, 2004; Akizawa et al., 2021).

The origin of plagioclase peridotite: the impact of late-stage low-pressure melting

The origin of plagioclase in plagioclase peridotite

Petrological observations of plagioclase in peridotite indicate that its origin involves subsolidus reactions from garnet and formation caused by melting at plagioclase peridotite stability conditions.

Ozawa and Takahashi (1995), Matsukage and Arai (1996) and Takahashi (1997, 2001) presented detailed petrological and mineralogical observation that could be explained by differences in the degree of melting and melt separation in partial melting, strongly supporting that melting had occurred in the Upper Zone (and also minor from the Lower Zone). Based on detailed textural and mineralogical analyses, four distinct modes of plagioclase occurrence are identified in plagioclase lherzolite of the MHL suite: fine-grained mineral aggregate, inclusion, isolated, and vein types. The distribution of these types is systematically controlled by the spatial variability in P-T trajectories during the ascent of the MHL suite. Plagioclase in the Lower Zone plagioclase lherzolite primarily occurs as fine-grained mineral aggregate derived from the subsolidus breakdown of garnet during decompression via spinel-pyroxene symplectite-bearing mineral aggregate. Locally, however, hydrous incipient melting at approximately 1000°C is evidenced by sodic plagioclase inclusions associated with Ti-pargasite within clinopyroxene porphyroclasts (Takahashi, 1997; 2001). In contrast, the Upper Zone plagioclase lherzolite records significant partial melting at temperatures of 1100-1170°C (Takahashi, 1997; 2001). In the Upper Zone, interstitial incipient melts successfully segregated from the peridotite matrix into macroscopic plagioclase-rich veins, locally forming interconnected networks (Takahashi, 1997; 2001).

Diversity of plagioclase peridotite

Plagioclase peridotites of the MHL suite can be classified into three petrogenetic types by integrating previous studies (Type I/II of Yoshida and Takahashi, 1997; N/E-types of Takazawa et al., 2000, DP/EP types of Yoshikawa and Nakamura, 2000, and TLP/MSP types of Malaviarachchi et al., 2008, 2010; Ranaweera et al., 2018) (Figs 6 and 7).

1) Normal-type plagioclase peridotite is consistent with residues of a MORB source like mantle (Type I of Yoshida and Takahashi, 1997; N-type of Takazawa et al., 2000; DP of Yoshikawa and Nakamura, 2000; DP-MSP of Ranaweera et al., 2018).
2) Enriched-type plagioclase peridotite is interpreted as residues that were subsequently overprinted by metasomatic fluids. The degree of enrichment was likely controlled by fluid flux variations within the mantle wedge, resulting in the LREE-enriched patterns ((La/Sm)N > 0.1 at Al_2O_3 wt. % < 3 %) characteristic of Enriched-type (Type II of Yoshida and Takahashi, 1997; E-type of Takazawa et al., 2000, EP of Yoshikawa and Nakamura, 2000, EP-MSP of Ranaweera et al., 2018).
3) Thin-layered-type plagioclase peridotite is interlayered with Type I mafic layers on a millimeter-to-centimeter scale. A distinguishing geochemical feature of the Thin-layered-type is its clinopyroxene exhibits higher Al and REE concentrations than those of other types (Fig. 13).

Yoshida and Takahashi (1997) revealed that the Upper Zone plagioclase lherzolites exhibit significantly higher compositional diversity compared to those in the Lower Zone, characterized by a distinct gap in TiO_2 concentrations that divides them into TiO_2 -rich (Type I) and TiO_2 -poor (Type II) groups. They suggested that the geochemical variability in the Upper Zone resulted from pervasive partial melting and variable extents of melt segregation during the ascent of the Horoman complex. In contrast, the Lower Zone plagioclase lherzolites appear to have escaped significant partial melting, largely preserving their primitive mantle compositions.

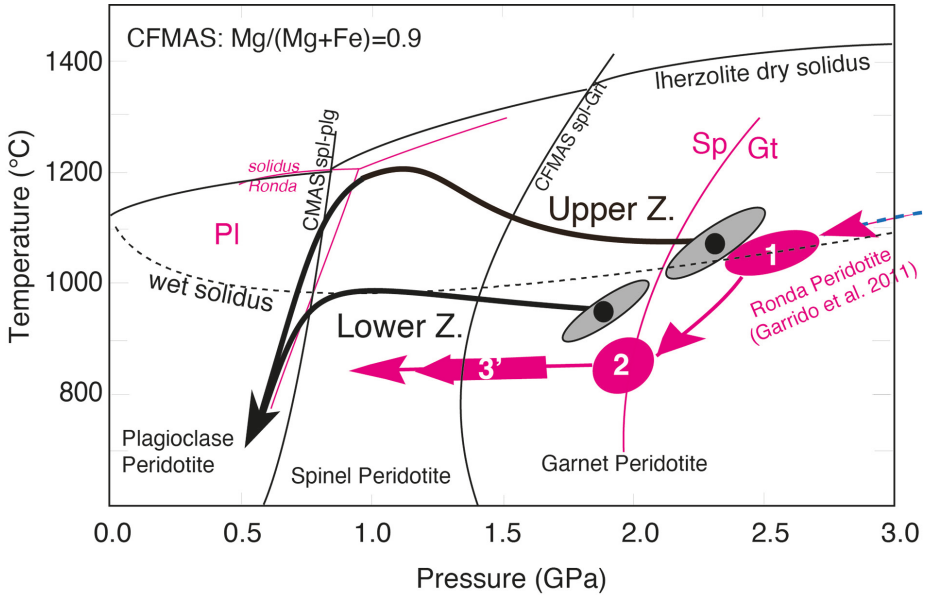

Fig. 14 - The estimated P-T trajectories for the Upper Zone (Upper Z.) and Lower Zone (Lower Z.) based on the MHL lherzolites (after Ozawa, 2004). The phase boundaries and dry solidus for the CaO-FeO-MgO-Al_2O_3-SiO_2 (CFMAS) system are shown in black (after Gasparik, 1987), alongside the wet solidus (after Kushiro et al., 1968). For comparative tectonic context, the P-T trajectory for the Ronda garnet peridotite (Spain) is shown in red (after Garrido et al., 2011).

Saal et al. (2001) suggested that mixing models using major and trace elements support that the Normal-type plagioclase lherzolites formed via melt-rock reaction or mixing between an Enriched-type plagioclase lherzolite and the Type I mafic layer. Malaviarachchi et al. (2010) suggested that the Thin-layered plagioclase peridotite represents a localized refertilization where highly depleted mantle residue interacted with an infiltrating melt forming Type I mafic layer.

Sm-Nd and Lu-Hf isochron data from the Thin-layered-type plagioclase peridotite and mafic layers indicated an age of approximately 300 Ma (Malaviarachchi et al., 2010): The Sm-Nd system yields an age of 257 ± 60 Ma, and the Lu-Hf system yields a consistent age of 313 ± 64 Ma. This 300 Ma age contrasts with the ~1 Ga Os isotope ages and 80 Ma Nd isotope ages reported for Type I and MHL plagioclase peridotites by Saal et al. (2001) and Takazawa et al. (1999), respectively. Such discrepancies in age may have been caused by late-stage partial melting events in fertile peridotites (i.e., plagioclase peridotites) and Type I mafic rocks.

Tasaka et al. (2024) conducted a detailed survey of a representative 3 x 70 m exposed section of the Thin-layered plagioclase peridotite and mafic layers in the Upper Zone. Quantitative EBSD analysis shows a distinct lithological control on deformation mechanisms. Spinel peridotites exhibit dislocation creep characterized by orthorhombic olivine CPOs, while the mafic layers undergo diffusion creep, evidenced by significant grain size reduction, weak CPOs, and grain-scale dissolution-precipitation features. The evolution of olivine crystal fabrics from (010) slip patterns to weak AG-type symmetries marks the transition from a melt-free to a melt-saturated rheological regime. They suggested that melts preferentially infiltrated the pre-existing tectonic foliation of peridotite host rocks, establishing a positive feedback loop between chemical reaction and mechanical weakening.

Enriched-type and Thin-layered-type plagioclase peridotites within the Upper Zone are inferred to have undergone varying degrees of interaction with melts associated with Type I mafic layers, or to have experienced partial melting of mafic layers and lherzolite under plagioclase peridotite stability conditions. Mafic layers associated with Thin-layered-type plagioclase peridotite are often less than 1 cm thick (Fig. 3b) and are generally interpreted as Type I layers; however, it is unclear whether these extremely thin mafic layers share the same origin as Type I layers. There may be multiple mafic layers with geochemical characteristics similar to those of the Type I mafic layer, which originated 1 Ga. If that is the case, it would be possible that there were some dating data available for the "Type I-like mafic layer." Consequently, a detailed characterization of Type I mafic layers is essential for a comprehensive understanding of the Horoman Peridotite Complex.

Layering of thin-layered-type plagioclase peridotite and as a signature of chaotic streamline mixing?

Toramaru et al. (1997, 2001) focused on outcrops in the Upper Zone, demonstrating the remarkable layering of MHL peridotites and Type I mafic layers (Thin-layered plagioclase peridotite and mafic layers), and pointed out a prominent geometric symmetrical arrangement centered on specific layers (Fig. 3b). They also pointed out that asymmetry of layering, characterized by subtle discrepancies in layer thickness between reciprocal sides of the center and occasional "layer defects" where corresponding lithologies are absent. They found an outcrop located approximately 3 km from this outcrop (Fig. 1a), which displays a striking similar but non-identical layered structure, underscoring the regional consistency of the structural mechanism. These outcrops are particularly noted for the frequent occurrence of paired mafic layers sandwiching thin horizons of plagioclase-free peridotite. These features can be explained by the iterative stretching and folding of a simple stratified precursor. This stretching and folding model with the spatial strain contrast can also explain the power-low frequency distribution of mafic layer widths.

A high-resolution 2D petrological-thermomechanical numerical model demonstrated that intense chaotic mixing leads to the mechanical stretching and duplication of lithological layers on scales ranging from 1 to 1000 meters (Gorczyk et al., 2007). Gorczyk et al. (2007) suggested that chaotic mixing process effectively transforms a simple initial stratigraphy into a "marble cake" structure characterized by high-frequency intercalations of mafic and ultramafic rocks, exhibiting a remarkable correlation with the layered structure of the Horoman Peridotite Complex.

These models strongly suggest that repetitive layered structures form from a simple lithological sequence through intense deformation, significantly influencing the investigation into the origin of the repetitive layering characteristic of the Horoman Peridotite Complex. However, tightly folded structures are not generally observed in the Horoman Complex (Takazawa, 1997; Morishita et al., 2006).

Unique geochemical reservoir

The Normal-type plagioclase peridotite (massive plagioclase lherzolites of Malaviarachichi et al., 2009), characterized by the lowest Pb isotope ratios ($^{206}Pb/^{204}Pb = 16.7$) ever reported for any mantle-derived material, are uniquely coupled with highly radiogenic Nd and Hf signatures (Fig. 15). These unradiogenic signatures plot significantly to the left of the 4.5 Gyr geochron in $^{207}Pb/^{204}Pb$ vs $^{206}Pb/^{204}P$ space, falling well below the established composition for the Depleted MORB Mantle (DMM). The initial Pb, Nd and Hf isotopic compositions of these samples nearly coincide with the predicted values for the average most-depleted MORB source mantle of 1 Ga. The Normal-type Plagioclase peridotites exhibit $^{87}Sr/^{86}Sr$ ratios that are markedly more depleted than the most depleted modern MORB mantle (Ranaweera et al., 2018). Low $^{87}Rb/^{86}Sr$ ratios of the Normal-type plagioclase peridotite suggest that virtually no radiogenic strontium has been accumulated since their initial formation. Geochemical modeling indicates that the calculated $^{87}Sr/^{86}Sr$ ratios for these samples at 1 Ga align almost perfectly with the most depleted MORB mantle of that period (Ranaweera et al., 2018). Malaviarachchi et al. (2008) and Ranaweera et al. (2018) suggest that the extremely low U/Pb and Th/Pb ratios required to produce such unradiogenic Pb over time may be linked to hydrothermal processes following melt extraction at a paleo-spreading ridge.

Unique component crucial for elucidating the history of the Horoman Complex: the BDH Suite and Type V mafic layer

The BDH suite

Petrology and mineral compositions of the BDH suite suggests that they are not residues of high-degree partial melting. The fact that the olivine NiO content rapidly decreases as the Fo content decreases supports their cumulus origin (Fig. 5). Mineralogical characteristics, high Fo olivine and high Cr# spinel (Fig. 5), indicate their origin in relation with the high-Mg andesite. Matsufuji et al. (2006) reported

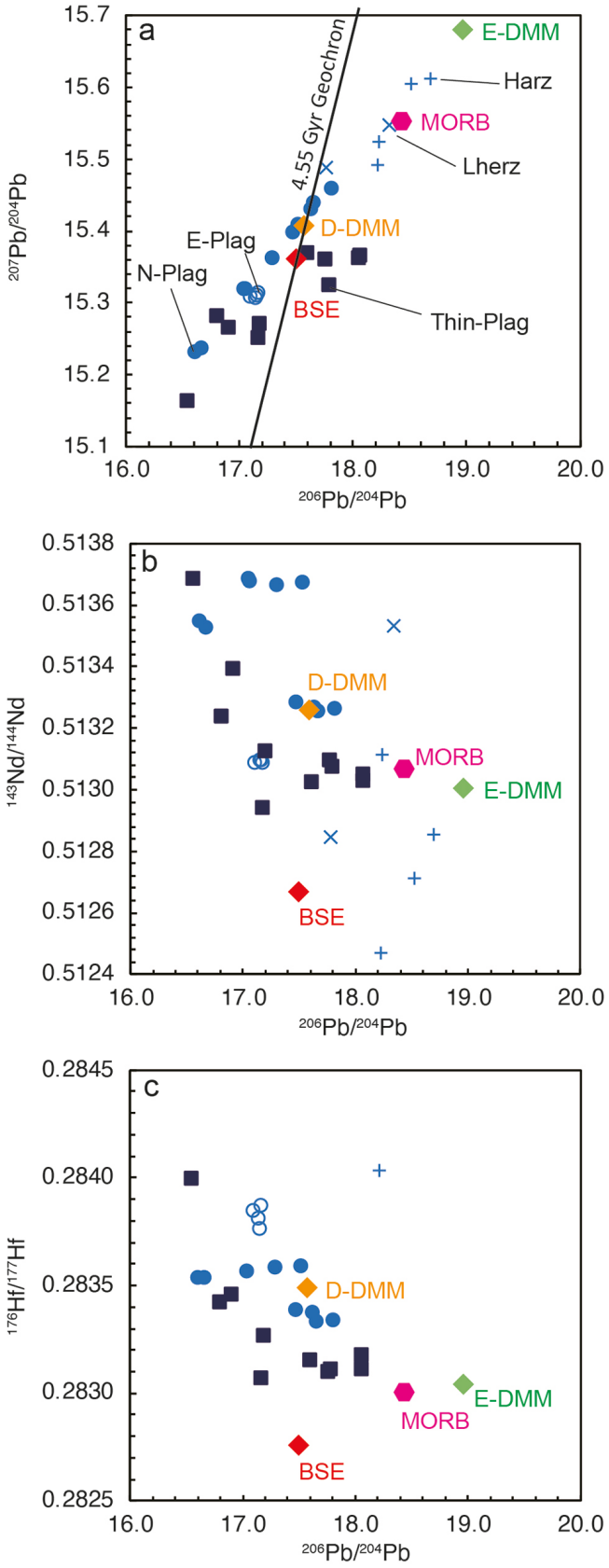

Fig. 15 - Isotopic systematics of the MHL peridotites. (a) $^{207}Pb/^{204}Pb$ versus $^{206}Pb/^{204}Pb$. The 4.55 giga year geochron is also shown. (b) $^{143}Nd/^{144}Nd$ versus $^{206}Pb/^{204}Pb$. (c) $^{176}Hf/^{177}Hf$ versus $^{206}Pb/^{204}Pb$. Data are from Malaviarachchi et al. (2008) and Ranaweera et al. (2018). Values of bulk silicate earth (BSE), depleted-depleted MORB mantle (D-DMM), enriched-depleted MORB mantle (E-DMM) and MORB are from Workman and Hart (2005) and Gale et al. (2013). N-Plag = Normal-type Plagioclase peridotite, E-Plag = Enriched-type Plagioclase peridotite, Thin-Plag= Thin layered-type Plagioclase peridotite, Lherz = Lherzolite, Harz = harzburgite.

clinopyroxene-bearing high-Mg and high-Cr peridotite variety within the BDH suite. This new type shows lower Cr# and higher Mg# and TiO_2 in spinel compared to other BDH peridotites, suggesting it formed later in the crystallization differentiation sequence of the BDH suite. Trace element compositions of clinopyroxene in this cpx-bearing one (Fig. 13) are analogous to clinopyroxenes associated with high-Mg andesite (boninite) formation (Takahashi, 1991, 1992; Matsufuji et al., 2006). Tasaka et al. (2025) suggested that the presence of strain-free pyroxenes (and pargasite, and spinel) with irregular sawtooth boundaries indicates they crystallized from melts, i.e., melt-rock interaction, along grain boundaries rather than through primary crystallization. Akizawa et al. (2021) proposed an alternative model for the BDH suite, suggesting that localized flux melting induced by slab-derived fluids generated peridotites characterized by high degrees of partial melting, i.e., BDH.

Both Type I and Type III mafic layers are observed in the BDH suite at the Nanagome outcrop (Fig. 3). The Type III mafic layer exhibits mineralogical characteristics similar to the Type I mafic layer, specifically in terms of its high TiO_2 content within the minerals, indicating a connection in terms of their petrological origin (Shiotani and Niita, 1997). These relationships indicate that the BDH suite was incorporated after the formation of the MHL-SDW suites and was intruded by melt associated with the Type I and Type III mafic layers (Matsufuji et al., 2006).

Detailed study on fluid inclusion relic (now mixture of hydrous minerals and carbonate minerals formed by interaction between trapped fluid and the host minerals at low-PT conditions) in dunite of the BDH suite was conducted by Hirai and Arai (1987). They revealed that the mineral assemblage filling these fluid inclusion relics is serpentine-magnesite-brucite. The relative amount is brucite = magnesite < serpentine, suggesting that the initially trapped H_2O-CO_2 fluid had an intermediate $CO_2/(H_2O+CO_2)$ ratio. It is interesting to note the detection of a small amount of chlorine from brucite in some inclusions, implying that the supplied fluid incorporated Cl. Detection of chlorine from fluid inclusion relic is consistent with the results of chlorine detection using the stepped crushing method (Kobayashi et al., 2017). Uniquely identified two distinct varieties of inclusions were identified in the Horoman olivine, suggesting that fluids with different compositions were supplied at two separate stages: a high-temperature stage and a low-temperature stage. This newer, lower-temperature type contains serpentine along with euhedral hexagonal minerals identified as calcite. The presence of calcite indicates a second fluid supply event occurring under different physicochemical conditions compared to the initial high-H_2O/intermediate-CO_2 event.

Type V mafic layer

The geochemical features of Type V strongly support a garnet-dominant rock as the source rock (Takazawa et al., 1999). The Type V exhibits a highly radiogenic Pb isotopic composition ($^{206}Pb/^{204}Pb$ = 21.194, $^{207}Pb/^{204}Pb$ = 15.781). This signature is interpreted as the result of radiogenic intergrowth over time within garnet-rich mineralogy, where high U/Pb and Th/Pb ratios were expected due to the preferential partitioning of U by garnet.

Mega olivine-bearing dunite formation event

Yoshikawa et al. (2019) investigated two discordant dunite channels (SPR and 1.6OL) found within a harzburgite of the

MHL suite. "Dunite channels" are characterized by extreme grain-size variations, notably the presence of very large olivine megacrysts (Fig. 3e), probably some exceeding 1.6 meters in length (Yoshikawa et al., 2019; Yamamoto et al., 2022). Non-destructive micro-Raman spectroscopy analysis confirmed that the olivine in dunite channel maintains a uniformity in crystallographic orientation along its entire length, with no evidence of abrupt discontinuities, and that Mg/Fe ratio (Mg#) exhibits a distinct, gradual compositional variation across the measured area, ranging from 86.5 to 93.0 (Yamamoto et al., 2022).

The channels are discordant to the existing layering of the host MHL harzburgite. Petrographic observations, coupled with mineral compositional data, support a replacive origin for the dunite channels, involving melt-rock interaction where orthopyroxene dissolution and subsequent olivine precipitation occurred. Olivine compositions exhibit high Mg# values (91.5-92.9) but display relatively low NiO contents compared to the typical mantle olivine array, consistent with derivation through melt-rock reaction (Yoshikawa et al., 2019). Spinel compositions within the dunite channels show elevated TiO_2 contents relative to the host harzburgite, also suggesting melt-rock interaction.

Clinopyroxenes within spinel-rich pyroxenite veinlets, which often crosscut the olivine megacrysts, and the neighboring harzburgite show trace element patterns highly enriched in LREEs relative to HREEs ($(La/Yb)_N$ = 2-5) (Fig. 13). The compositions of the melts in equilibrium with these clinopyroxenes share key characteristics: LREE enrichment, HREE depletion, positive Sr anomalies, and significant depletion in high field strength elements (HFSEs) and Pb. This trace element signature is inconsistent with other major mafic layers (Types I and II mafic layers), indicating a distinct magmatic event.

The Sr and Nd isotopic ratios of clinopyroxenes from the pyroxenite veinlets in dunite channels are broadly similar to MORB, yet they are distinct from one another, confirming the involvement of different melts. The overall trace element modeling indicates that the magmas were derived from a depleted MORB-source mantle that had been metasomatized by components originating from a subducting oceanic slab.

Rb-Sr systematics on clinopyroxene-orthopyroxene pairs suggests a crystallization age of approximately 52 ± 19 Ma for the pyroxenite veinlets. This Eocene age places the formation of these discordant dunite channels as a relatively late-stage event in the Horoman Complex history.

Modal Metasomatism: 23 Ma "Alkali" metasomatism

Niida (1975a) first reported the presence of TiO_2-rich phlogopite from the HML lherzolite. Arai and Takahashi (1989) and Takahashi et al. (1989) suggested that interstitial grains or concentrated veinlets of phlogopite and amphibole in the MHL suite represent evidence of "alkali" metasomatism. Phlogopite exhibits significant compositional variability, a wide range of TiO_2 contents and K/(K+Na) ratio within individual veins. The observed heterogeneity in phlogopite composition, particularly the fluctuation in K/(K+Na) ratios, is interpreted as the result of fractionation of metasomatic fluids derived during the fractional crystallization of an alkali basaltic magma.

The groundbreaking study on the timing and genesis of alkali metasomatism for the formation of phlogopite and amphibole in the MHL suite was conducted by Yoshikawa and Nakamura (1993). Detailed Rb-Sr isotope systematics on mineral separates (phlogopite, clinopyroxenes, orthopyroxene) and whole rock from a phlogopite-bearing spinel lherzolite of the MHL suite yield a highly coherent isochron age of 23.0 ± 1.2 Ma (2σ) with an initial $^{87}Sr/^{86}Sr$ ratio of 0.703871 ± 0.000007 (2σ). This age is also consistent with the ^{40}Ar-^{39}Ar analysis of phlogopite separated from a phlogopite-bearing plagioclase lherzolite yielding a plateau age of 20.6 ± 0.5 Ma (Kaneoka et al., 2001). The estimated initial $^{87}Sr/^{86}Sr$ ratio (approximately 0.7039) is significantly higher for phlogopite-bearing peridotite than that of phlogopite-free spinel lherzolites (<0.7028), requiring the metasomatic fluid to have an exotic origin, such as dehydration of subducted oceanic sediments (Yoshikawa and Nakamura, 1993). The inverse-isochron plot for the phlogopite indicated an initial $^{40}Ar/^{36}Ar$ ratio of the phlogopite close to the present atmospheric ratio, suggesting that the metasomatic agent had been affected by components in equilibrium with the atmosphere (Kaneoka et al., 2001).

Although these age data were obtained from phlogopite-rich veinlets in the MHL suite, it should be noted that phlogopite (and/or amphibole) are frequently observed in many rock type. This late-stage "alkaline metasomatism" may have a more widespread impact on all types of suites as well as mafic layers than we realize.

SUMMARY AND CONCLUDING REMARKS

We summarize the lithological sequence of the Horoman Peridotite Complex, integrating field and petrological observations (Fig. 16). Both SDW-MHL suite groups (including protolith of the Type II mafic layer) formed in the earliest stage. Ascent and partial melting of a MORB-source mantle near the garnet-spinel transition at c.a. 1 Ga produced a residual mantle exhibiting variable degrees of partial melting. Note that the protolith of the Type II mafic layer formed as gabbro (plagioclase-olivine stability conditions, i.e., < 0.8 GPa). The crystallization of Type II layers and the formation of the SDW took place within the shallow oceanic upper mantle. The Type II mafic layers, i.e. all the SDW-MHL suites, were metamorphosed under garnet peridotite stability conditions. The BDH suite, derived from high-Mg andesitic melts indicative of an arc setting, were incorporated into the MHL suite as exotic blocks. The protolith of the Type I (and Type III) mafic layer intruded as garnet pyroxenite into the MHL (and BDH as Type III mafic layers) suites. Mega olivine-bearing dunite channel was formed by melt-rock interaction at ca. 50 Ma. All lithological units, including the BDH blocks entrained in the SDW-MHL suite and the associated mafic layers, ascended from the garnet to the plagioclase peridotite stability field. During ascent, partial melting of the MHL plagioclase lherzolite (and the Type I mafic layers) produced plagioclase-rich veins that reacted with the surrounding peridotites. All lithologies, including the mafic layers, underwent multiple stages of slab-derived metasomatism, culminating in the formation of phlogopite and pargasite at ca. 23 Ma. Conversely, the less metasomatized MHL plagioclase peridotites preserve unique isotopic compositions dating back ~1 Ga.

Key outstanding questions concerning the evolutionary history of the Horoman Peridotite Complex include:

The origin of the BDH suite and the mechanisms responsible for the incorporation of these distinctive blocks into the main MHL suite.

The origin of Type I mafic layers, particularly the thin layers hosted within plagioclase peridotite, and their relationship to the partial melting of both peridotite and mafic lithologies under plagioclase peridotite stability conditions.

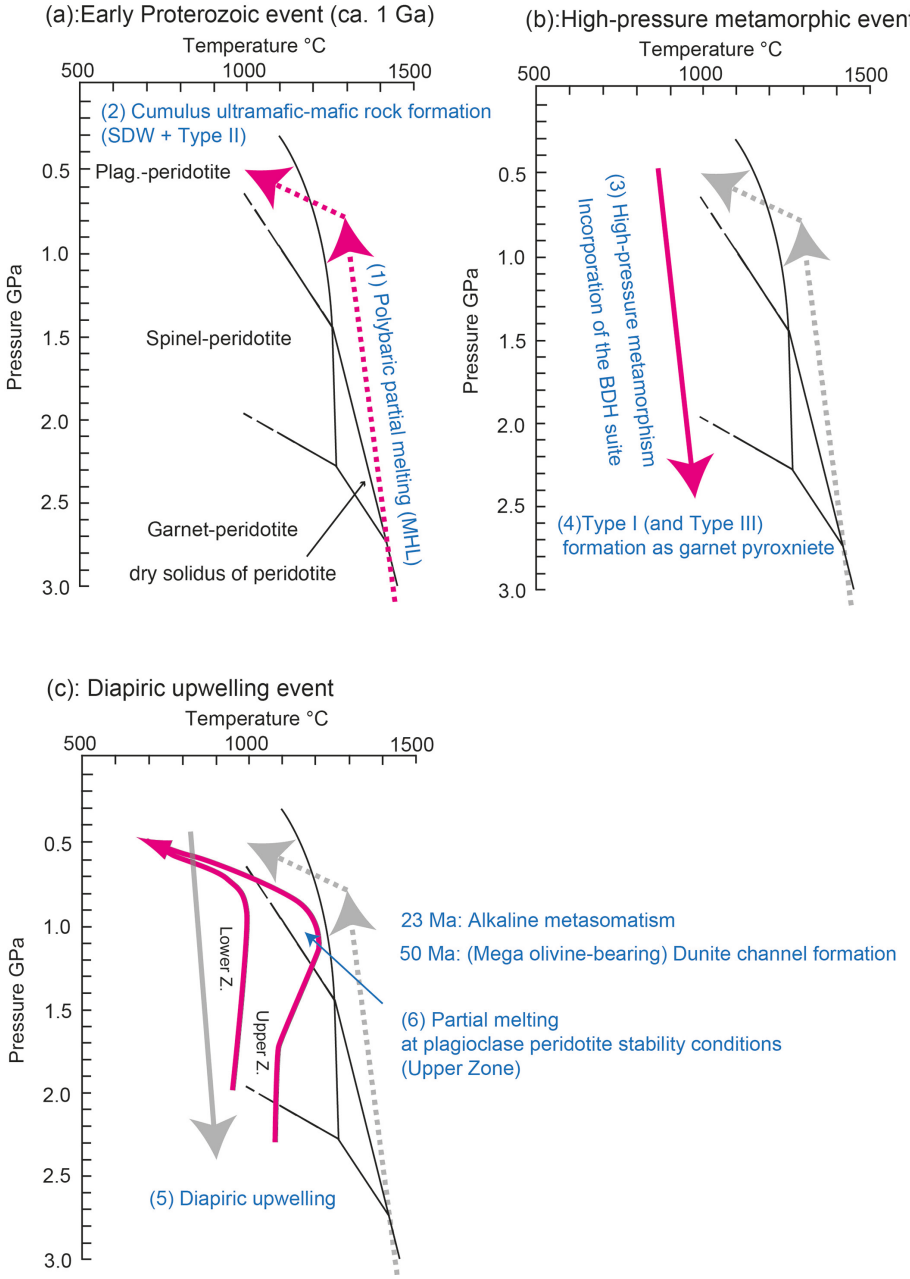

Fig. 16 - Conceptual Pressure-Temperature-Time evolutionary history of the Horoman Peridotite Complex. (a) Early Proterozoic event (ca. 1 Ga): The MHL residual suite was generated through the polybaric partial melting of a MORB-source mantle, spanning the transition from garnet- to spinel-peridotite stability fields. Contemporaneously, the SDW suite and the protoliths of Type II mafic layers (plagioclase-bearing gabbroic cumulates) formed within a shallow oceanic upper mantle setting at pressures < 0.8 GPa. (b) High-pressure metamorphism, incorporation of the BDH suite, and Type I mafic layer formation: The primary MHL-SDW suites including Type II mafic layer underwent high-pressure metamorphism under garnet peridotite stability conditions (3), as evidenced by corundum and garnet-origin symplectites in the SDW and Type II mafic layers. During this stage (3), the exotic BDH blocks (likely arc-derived) were probably tectonically incorporated into the MHL-SDW sequence. Melts forming the Type I and Type III mafic layers intruded the MHL and BDH suites as garnet pyroxenites while the complex remained within the garnet peridotite stability conditions (4). These intrusions postdate the initial formation of the residual MHL suite. (c) Diapiric upwelling and metasomatism: All lithological suites (MHL-SDW-BDH suites and associated mafic layers) underwent adiabatic upwelling from garnet peridotite stability conditions to plagioclase peridotite stability conditions (5). Partial melting of fertile plagioclase lherzolites and Type I mafic layers in the Upper Zone produced plagioclase-rich segregation veins that crosscut the primary foliation (6). Key other events during this ascent include: formation of mega-olivine dunite channels via melt-rock interaction at ca. 50 Ma, and ca. overprinting by slab-derived alkali metasomatism, resulting in the localized formation of phlogopite, at ca. 23 Ma. Note that the MHL suite as well as mafic layers likely underwent multiple episodes of metasomatic overprinting via the infiltration of metasomatic agents. These processes induced localized refertilization and abrupt geochemical discontinuities within otherwise continuous lithological sequences, although the precise geochronology of these events remains poorly constrained.

Spatial dimensions of geochemical heterogeneities of mantle, such as unradiogenic Pb domain, and the mechanisms governing their episodic formation and giga-year preservation.

ACKNOWLEDGEMENTS

The authors would like to express their profound gratitude to Kiyoaki Niida, Masaaki Obata, Shoji Arai, and Fred Frey for their invaluable mentorship and expert guidance. Their pioneering insights into the lithological and petrological evolution of the Horoman Peridotite Complex provided the essential foundation for the conceptual framework. The authors are also grateful to Kazuki Matsuyama and Ryoko Nagashima for generously providing the lithological map and photo images of symplectitic aggregate of the Horoman Peridotite Complex, respectively. The manuscript has been significantly improved based on the peer review comments from Valentin Basch and Nori Akizawa. This study was supported by a Grants-in-Aid for Scientific Research from the Ministry of Education, Culture, Sports, Science and Technology of Japan to ET (Nos. 20H02005, 25K07436).

ONLINE SUPPLEMENTARY MATERIAL

Supplementary data to this article are available online at https://doi.org/10.4454/ofioliti.v51i2.590

REFERENCES

Akamatsu Y., Hatakeyama K. and Katayama I., 2019. Contrasting dilatant behaviors of mafic and ultramafic rocks based on triaxial deformation experiments. J. Mineral. Petrol. Sci., 114: 79-86. doi:10.2465/jmps.181120

Akizawa N., Ozawa K. and Yoshikawa M., 2021. Decoding pressure-temperature-deformation history of the mantle: Critical re-

view on the Horoman peridotite complex and new proposals. J. Geol. Soc. Japan, 127: 269-291. doi:10.5575/geosoc.2021.0011

Anguelova, M., Fehr, M.A., Takazawa, E., Schönbächler, M., 2022. Titanium isotope heterogeneity in the Earth's mantle: a case study of the Horoman peridotite massif. Geochim. Cosmochim. Acta 335: 356-368. doi:10.1016/j.gca.2022.06.035

Arai S., 1994. Characterization of spinel peridotites by olivine-spinel compositional relationships: Review and interpretation. Chem. Geol., 113: 191-204. doi:10.1016/0009-2541(94)90066-3

Arai S. and Takahashi N., 1989. Formation and compositional variation of phlogopites in the Horoman peridotite complex, Hokkaido, northern Japan: implications for origin and fractionation of metasomatic fluids in the upper mantle. Contrib. Mineral. Petrol., 101: 165-175. doi:10.1007/BF00375303

Arai S., Hoshikawa C., Miura M., Ando J.-I., Ishimaru S., Mochizuki N. and Tamura A., 2021. Dehydrogenation of deep-seated hydrous olivine in "black-colored" dunites of arc origin. Lithos, 384-385: 105967. doi:10.1016/j.lithos.2021.105967

Arita K., Toyoshima T., Owada M., Miyashita S. and Jolivet L., 1986. Tectonic movements of the Hidaka metamorphic belt, Hokkaido, Japan. Monogr. Assoc. Geol. Collab. Japan, 31: 247-263.

Gale A., Dalton, C. A., Langmuir C. H., Su Y. and Schilling J.-G., 2013. The mean composition of ocean ridge basalt. Geochem. Geophys. Geosyst., 14: 489-518. doi:10.1002/ggge.20038

Garrido C. J. and Bodinier, J.-L., 1999. Diversity of Mafic Rocks in the Ronda Peridotite: Evidence for Pervasive Melt-Rock Reaction during Heating of Subcontinental Lithosphere by Upwelling Asthenosphere. Jour. Petrol. 40: 729-754. doi:10.1093/petroj/40.5.729

Garrido C. J., Gueydan F., Booth-Rea G., Precigout J., Hidas K., Padrón-Navarta J. A., et al. (2011). Garnet lherzolite and garnet-spinel mylonite in the Ronda peridotite: Vestiges of Oligocene backarc mantle lithospheric extension in the western Mediterranean. Geology 39: 927-930. doi:10.1130/G31760.1

Gasparik T., 1987. Orthopyroxene thermobarometry in simple and complex systems. Contrib. Mineral. Petrol., 96: 357-370. doi:10.1007/BF00371254

Ichihara H., Mogi T., Tanimoto K., Yamaya Y., Hashimoto T., Uyeshima M. and Ogawa Y., 2016. Crustal structure and fluid distribution beneath the southern part of the Hidaka collision zone revealed by 3-D electrical resistivity modeling. Geochem. Geophys. Geosyst., 17: 1480-1491. doi:10.1002/2015GC006240

Igi S. (1953). Petrographical Studies on the Peridotite in the Horoman Region at the Southerr end of the Hidaka Mountain Range, Hokkaido. Jour. Geol. Soc. Japan, 59: 111-121. doi:10.5575/geosoc.59.111

Ikehata K. and Hirata T., 2012. Copper isotope characteristics of copper-rich minerals from the Horoman peridotite complex, Hokkaido, northern Japan. Econ. Geol., 107: 1489-1497. doi:10.2113/econgeo.107.7.1489

Imai N., Terashima S., Itoh S., and Ando, A., 1995. 1994 compilation values for GSJ reference samples, "Igneous rock series". Geochem. Jour., 29: 91-95. doi:10.2343/geochemj.29.91

Kaneoka I., Takahashi N. and Arai S., 2001. 40Ar-39Ar analysis of phlogopite in the Horoman Peridotite Complex, Hokkaido, Japan and implications for its origin. Isl. Arc, 10: 22-32. doi:10.1046/j.1440-1738.2001.00290.x

Kitakaze A., 1998. Sulfide minerals from the Horoman peridotite, Hokkaido, Japan. Jour. Mineral. Petrol. Econ. Geol., 93: 369-379. doi:10.2465/ganko.93.369

Kitakaze A., 2008. Sugakiite, Cu(Fe,Ni)8S8, a new mineral species from Hokkaido, Japan. Can. Mineral. 46: 263-267. doi:10.3749/canmin.46.1.263

Kitakaze A., Itoh H., and Komatsu R., 2011. Horomanite, (Fe,Ni,Co,Cu)9S8, and samaniite, Cu2(Fe,Ni)7S8, new mineral species from the Horoman peridotite massif, Hokkaido, Japan. Jour. Mineral. Petrol. Sci. 106: 204-210. doi:10.2465/jmps.110502

Kobayashi M., Sumino H., Nagao K., Ishimaru S., Arai S., Yoshikawa M., et al., 2017. Slab-derived halogens and noble gases illuminate closed system processes controlling volatile element transport into the mantle wedge. Earth Planet. Sci. Lett. 457: 106-116. doi:10.1016/j.epsl.2016.10.012

Kogiso T., Suzuki K., Suzuki T., Shinotsuka K., Uesugi K., Takeuchi A. and Suzuki Y., 2008. Detecting micrometer-scale platinum group minerals in mantle peridotite with microbeam synchrotron radiation X-ray fluorescence analysis. Geochem. Geophys. Geosystem., 9: 1-9. doi:10.1029/2007GC001888

Komatsu M., Miyashita S., Maeda J., Osanai Y., Toyoshima T., Motoyoshi Y. and Arita K., 1982. Petrological constitution of the continental type crust upthrust in the Hidaka belt, Hokkaido. J. Japan. Assoc. Mineral. Petrol. Econ. Geol., 3: 229-238. doi:10.11467/ganko1941.Special3.229

Komatsu M. and Nochi M., 1966. Ultrabasic Rocks in the Hidaka Metamorphic Belt, Hokkaido, Japan I -Mode of Occurrence of the Horoman Ultrabasic Rocks-. Earth Sci. (Chikyu Kagaku), 87: 21-29. doi:10.15080/agcjchikyukagaku.1966.87_21

Komatsu M., Toyoshima T., Osanai Y. and Arai M., 1994. Prograde and anatectic reactions in the deep arc crust exposed in the Hidaka metamorphic belt, Hokkaido, Japan. Lithos, 33: 31-49. doi:10.1016/0024-4937(94)90053-1

Kushiro I. and Yoder H. S., 1966. Anorthite-forsterite and anorthite-enstatite reactions and their bearing on the basalt-eclogite transformation. J. Petrol., 7: 337-362. doi:10.1093/petrology/7.3.337

Kushiro I., Syono Y. and Akimoto S., 1968. Melting of a peridotite nodule at high pressures and high water pressures. J. Geophys. Res., 73: 6023-6029. doi:10.1029/JB073i018p06023

Lai Y.-J., Pogge von Strandmann P. A. E., Dohmen R., Takazawa E. and Elliott T., 2015. The influence of melt infiltration on the Li and Mg isotopic composition of the Horoman Peridotite Massif. Geochim. Cosmochim. Acta, 164: 318-332. doi:10.1016/j.gca.2015.05.028

Malaviarachchi S. P. K., Makishima A., Tanimoto M., Kuritani T. and Nakamura E., 2008. Highly unradiogenic lead isotope ratios from the Horoman peridotite in Japan. Nat. Geosci., 1: 859-863. doi:10.1038/ngeo343

Malaviarachchi S. P. K., Makishima A. and Nakamura E., 2010. Melt-peridotite reactions and fluid metasomatism in the upper mantle, revealed from the geochemistry of peridotite and gabbro from the Horoman Peridotite Massif, Japan. J. Petrol., 51: 1417-1445. doi:10.1093/petrology/egq024

Matsufuji Y., Arai S., Morishita T. and Ishida Y., 2006. Petrology of exotic high-Mg, Cr peridotite bodies in the Horoman Peridotite Complex, Japan. Japan. Mag. Mineral. Petrol. Sci., 35: 231-243. doi:10.2465/ganko.101.231

Matsukage K. and Arai S., 1996. Mode of occurrence of plagioclase-rich segregation in the Horoman peridotite. Sci. rep. Kanazawa Univ., 41: 47-67.

Matsuyama K. and Michibayashi K., 2023. Variation in olivine crystal-fabrics and their seismic anisotropies in the Horoman peridotite complex, Hokkaido, Japan. J. Geodyn., 158: 102006. doi:10.1016/j.jog.2023.102006

Matsuyama K. and Michibayashi K., 2024. Structural evolution of the Horoman peridotite complex in conjunction with the formation of the Hidaka Metamorphic Belt, Hokkaido. Tectonophysics, 892: 230535. doi:10.1016/j.tecto.2024.230535

Matsuyama K. and Michibayashi K., 2025. Deformation structure of the Horoman peridotite complex: Overview of microstructural and petrological variation and beyond. J. Geol. Soc. Japan, 131: 521-535. doi:10.5575/geosoc.2024.0044

McDonough W. and Sun S., 1995: The composition of the Earth. Chem. Geol., 120, 223-253. doi:10.1016/0009-2541(94)00140-4

Mikuni K., Terashima S., Okai T., Kubota R., Nakamura A., and Ohta A., 2025. Five new geochemical reference materials of igneous rocks: Andesite JA-2a, granite JG-2a, granodiorite JG-3a, gabbro JGb-1a, and peridotite JP-2. Geochem. Jour. doi:10.2343/geochemj.gj25016

Miura Y. and Nagao K., 1991. Noble gases in six GSJ igneous rock samples. Geochem. Jour. 25: 163-171. doi:10.2343/geochemj.25.163

Morishita R., 1998. A mathematical modling of pattern-generation in rock textures and its application to natural rock textures. Forma, 13: 179-197.

Morishita T., 1998. Possible pseudotachylyte from the Horoman peridotite complex of the Hidaka belt, Hokkaido, northern Japan. Jour. Geol. Soc. Japan, 104: 18-23. doi:10.5575/geosoc.104.18

Morishita T., 2000a. Petrographycal characteristics of a serpentinized cataclasite boulder in the Horoman peridotite complex. Jour. Geol. Soc. Japan, 106: 223-233. doi:10.5575/geosoc.106.223

Morishita T., 2000b. Three-dimensional microstructure of symplectite minerals in the Horoman peridotite: a preliminary analysis. J. Geol. Soc. Japan, 106: 800-811. doi:10.5575/geosoc.106.800

Morishita T. and Arai S., 1997. Diversity of occurrence of symplectite in the Horoman peridotite complex if the Hidaka belt, Hokkaido, northern Japan, and its bearing on the P-T history. Mem. Geol. Soc. Japan, 47: 149-162.

Morishita T. and Arai S., 2001. Petrogenesis of corundum-bearing mafic rock in the Horoman Peridotite Complex, Japan. J. Petrol., 42: 1279-1299. doi:10.1093/petrology/42.7.1279

Morishita T. and Arai S., 2003. Evolution of spinel-pyroxene symplectite in spinel-lherzolites from the Horoman Complex, Japan. Contrib. Mineral. Petrol., 144: 509-522. doi:10.1007/s00410-002-0414-1

Morishita T., Arai S. and Green D. H., 2003a. Evolution of low-Al orthopyroxene in the Horoman peridotite, Japan: an unusual indicator of metasomatizing fluids. J. Petrol., 44: 1237-1246. doi:10.1093/petrology/44.7.1237

Morishita T., Arai S. and Green D. H., 2004. Possible non-melted remnants of subducted lithosphere: experimental and geochemical evidence from corundum-bearing mafic rocks in the Horoman Peridotite Complex, Japan. J. Petrol., 45: 235-252. doi:10.1093/petrology/egh002

Morishita T., Arai S. and Ishida Y., 2007. Occurrence and chemical composition of amphiboles and related minerals in corundum-bearing mafic rock from the Horoman Peridotite Complex, Japan. Lithos, 95: 425-440. doi:10.1016/j.lithos.2006.09.002

Morishita T. and Kodera T., 1998. Finding of corundum-bearing gabbro boulder possible derived from the Horoman peridotite complex, Hokkaido, northern Japan. J. Mineral. Petrol. Econ. Geol., 93: 52-63. doi:10.2465/ganko.93.52

Morishita T., Tsuchiyama A., Nakano T. and Uesugi K., 2003b. Observations of three-dimensional microstructures of symplectite minerals in the Horoman peridotite complex using a high-resolution X-ray CT system at SPring-8. J. Geol. Soc. Japan, 109: III-IV. doi:10.5575/geosoc.109.3_III

Morishita T., Takazawa E., Arai S., Obata M., Kodera T. and Gervilla F., 2006. Corundum-bearing mafic granulites in the Horoman (Japan) and Ronda (Spain) Peridotite Massifs: Possible remnants of recycled crustal materials in the mantle. Island Arc 15: 2-3. doi:10.1111/j.1440-1738.2006.00517.x

Nagasaki, H., 1966. A layered ultrabasic complex at Horoman, Hokkaido, Japan. Jour. Fac. Sci. Univ. Tokyo, 16: 313-346.

Niida K., 1974. Structure of the Horoman ultramafic massif of the Hidaka metamorphic belt in Hokkaido, Japan. J. Geol. Soc. Japan, 80: 31-44. doi:10.5575/geosoc.80.31

Niida K., 1975a. Phlogopite from the Horoman Ultramafic Rocks. J. Fac. Sci. Hokkaido Univ., Ser. IV, 16: 511-518.

Niida K., 1975b. Textures and olivine fabrics of the Horoman ultramafic rocks, Japan. J. Japan. Assoc. Min. Petr. Econ. Geol., 70: 265-285. doi:10.2465/ganko1941.70.265

Niida K., 1984. Petrology of the Horoman ultramafic rocks in the Hidaka metamorphic belt, Hokkaido, Japan. J. Fac. Sci. Hokkaido Univ., Ser. IV, 21: 197-250.

Niida K. and Takazawa E., 2007. Origin of layering observed in the Horoman peridotite complex. J. Geol. Soc. Japan, 113: 167-184. doi:10.5575/geosoc.113.167

Niida K., Takahashi N., Takazawa E., Sawaguchi T., Morishita T., Ozawa K. and Obata M. (Eds.), 2002. Guide Book for Field Excursion to the Horoman Peridotite Complex. Samani, 98p.

Obata M. and Nagahara N., 1987. Layering of alpine-type peridotite and the segregation of partial melt in the upper mantle. J. Geophys. Res. B: Solid Earth, 92: 3467-3474. doi:10.1029/JB092iB05p03467

Obata M. and Takazawa, E., 2004. Compositional continuity and discontinuity in the Horoman peridotite, Japan, and its implication for melt extraction processes in partially molten upper mantle. J. Petrol., 45: 223-234. doi:10.1093/petrology/egg106

Obata M., Morishita R. and Tanaka K., 1997. The microstructure of pyroxene-spinel symplectite from the Horoman peridotite and its formation processes. Mem. Geol. Soc. Japan, 47: 163-171.

Odashima N., Morishita T., Ozawa K., Nagahara H., Tsuchiyama A. and Nagashima R., 2008. Formation and deformation mechanisms of pyroxene-spinel symplectite in an ascending mantle, the Horoman peridotite complex, Japan: An EBSD study. J. Mineral. Petrol. Sci., 103: 1-15. doi:10.2465/jmps.103.1

Osanai Y., Owada M. and Kawasaki T., 1992. Tertiary deep crustal ultrametamorphism in the Hidaka metamorphic belt, northern Japan. J. Metamorph. Geol., 10: 401-414. doi:10.1111/j.1525-1314.1992.tb00093.x

Ozawa K., 1997. P-T history of an ascending mantle peridotite constrained by Al zoning in orthopyroxene: a case study in the Horoman peridotite complex. Mem. Geol. Soc. Japan, 47: 107-122.

Ozawa K., 2001. Mass balance equations for open magmatic systems: trace element behavior and its application to open system melting in the upper mantle. J. Geophys. Res. B: Solid Earth, 106: 13407-13434. doi:10.1029/2000JB900455

Ozawa K., 2004. Thermal history of the Horoman peridotite complex: a record of thermal perturbation in the lithospheric mantle. J. Petrol., 45: 253-273. doi:10.1093/petrology/egg108

Ozawa K. and Takahashi N., 1995. P-T history of a mantle diapir: the Horoman peridotite complex, Hokkaido, northern Japan. Contrib. Mineral. Petrol., 120: 223-248. doi:10.1007/BF00306506

Ranaweera L.V., Ota T., Moriguchi T., Tanaka R. and Nakamura E., 2018. Circa 1 Ga sub-seafloor hydrothermal alteration imprinted on the Horoman peridotite massif. Sci. Rep., 8: 9887. doi:10.1038/s41598-018-28219-x

Saal A. E., Takazawa E., Frey F. A., Shimizu N. and Hart S. R., 2001. Re-Os isotopes in the Horoman Peridotite: evidence for refertilization? J. Petrol., 42: 25-37. doi:10.1093/petrology/42.1.25

Sawaguchi T., 2004. Deformation history and exhumation process of the Horoman peridotite complex, Hokkaido, Japan. Tectonophysics, 379: 109-126. doi:10.1016/j.tecto.2003.10.024

Sawaguchi, T. and Takagi, H., 1997. Inverted ductile shear movement of the Horoman peridotite complex in the Hidaka metamorphic belt, Japan. Mem. Geol. Soc. Japan, 47: 193-208.

Sawaguchi T., Goto K. and Takagi H., 2001. Elongated orthopyroxene porphyroclasts as a shear sense indicator and kinematic history of the Horoman peridotite complex. J. Geol. Soc. Japan, 107: 165-178. doi:10.5575/geosoc.107.165

Shiotani Y. and Niida K., 1997. Origin of mafic layers in the Horoman peridotite complex. Mem. Geol. Soc. Japan, 47: 123-137.

Takahashi E., Uto K., Schilling J.G., 1987. Primary magma compositions and Mg/Fe ratios of their mantle residues along Mid Atlantic Ridge. Tech. Rep. ISEI, Okayama Univ. 10, 9-14.

Takahashi N., 1991. Origin of three peridotite suite from Horoman peridotite complex, Hokkaido, Japan; Melting, melt segregation and solidification processes in the upper mantle. J. Mineral. Petrol. Econ. Geol., 86: 199-215. doi:10.2465/ganko.86.199

Takahashi N., 1992. Evidence for melt segregation towards fractures in the Horoman mantle peridotite complex. Nature, 359: 52-55. doi:10.1038/359052a0

Takahashi N., 1997. Incipient melting of mantle peridotites observed in the Horoman and Nikanbetsu peridotite complexes. J. Mineral. Petrol. Econ. Geol., 92: 1-24. doi:10.2465/ganko.92.1

Takahashi N., 2001. Origin of plagioclase lherzolite from the Nikanbetsu Peridotite Complex. J. Petrol., 42: 39-54. doi:10.1093/petrology/42.1.39

Takahashi N. and Arai S., 1989. Textual and chemical features of chromian spinel-pyroxene symplectites in the Horoman peridotites, Hokkaido, Japan. Sci. Rep. Inst. Geosci. Univ. Tsukuba Sec. B, 10: 45-55.

Takahashi N., Arai S., and Murota Y., 1989. Alkali metasomatism in peridotite complexes from the Hidaka belt, Hokkaido, northern Japan. Jour. Geol. Soc. Japan, 95: 311-329. doi:10.5575/geosoc.95.311

Takazawa E., 1996. Geodynamic evolution of the Horoman peridotite, Japan: Geochemical study of lithospheric and asthenosperic processes. PhD thesis, Massachusetts Institute Technology: 562pp.

Takazawa E., Frey F. A., Shimizu N. and Obata M., 1996. Evolution of the Horomn Peridotite (Hokkaido, Japan): Implications from pyroxene compositions. Chem. Geol., 134: 3-26. doi:10.1016/S0009-2541(96)00083-6

Takazawa E., Frey F.A., Shimizu N. and Obata M., 2000. Whole-rock compositional variations in an upper mantle peridotite (Horoman, Hokkaido, Japan): Are they consistent with partial melting hypothesis? Geochim. Cosmochim. Acta, 64: 695-716. doi:10.1016/S0016-7037(99)00346-2

Takazawa E., Frey F.A., Shimizu N., Obata M. and Bodinier J.-L., 1992. Geochemical evidence for melt migration and reaction in the upper mantle. Nature, 359: 55-58. doi:10.1038/359055a0

Takazawa E., Frey F.A., Shimizu N., Obata M. and Bodinier J.-L., 1999. Polybaric petrogenesis of mafic layers in the Horoman Peridotite Complex, Japan. J. Petrol., 40: 1827-1851. doi:10.1093/petrology/40.12.1827

Tasaka M., Hihara A., Kurihara K., Taniuchi H. and Kawamoto T., 2024. Deformation and melt-rock interaction in the upper mantle: Insights from the layered structure of the Horoman peridotite, Japan. Tectonophysics, 890: 230508. doi:10.1016/j.tecto.2024.230508

Tasaka M., Hihara A., Kurihara K., Taniuchi H. and Kawamoto T., 2025. Effects of melt-rock interactions on forearc mantle deformation as evidenced by banded dunite-harzburgite in the Horoman peridotite complex, Japan. Lithos 518-519: doi:10.1016/j.lithos.2025.108316

Tazaki K., Ito E. and Komatsu M., 1972. Experimental study on a pyroxene-spinel symplectite at high pressures and temperatures. J. Geol. Soc. Japan, 78: 347-354. doi:10.5575/geosoc.78.347

Toramaru A., 1997. Origin of layered structure of the Horoman ultramafic complex. Mem. Geol. Soc. Japan, 47: 185-192.

Toramaru A., Takazawa E., Morishita T. and Matsukage K., 2001. Model of layering formation in a mantle peridotite (Horoman, Hokkaido, Japan). Earth Planet. Sci. Lett., 185: 299-313. doi:10.1016/S0012-821X(00)00373-1

Tsumura N., Ikawa H., Ikawa T., Shinohara M., Ito T., Arita K., Moriya T., Kimura G., and Ikawa T., 1999. Delamination-wedge structure beneath the Hidaka Collision Zone, Central Hokkaido, Japan inferred from seismic reflection profiling. Geophys. Res. Lett., 26: 1057-1060. doi:10.1029/1999GL900142

Workman R. and Hart S., 2005. Major and trace element composition of the depleted MORB mantle (DMM). Earth Planet. Sci. Lett., 231: 53-72. doi:10.1016/j.epsl.2004.12.010

Yamamoto A., Yamada K., Saito M. and Ishikawa H., 2001. Gravity anomaly around the Horoman peridotite region, central Hokkaido, Japan. Geophy. Bull. Hokkaido Univ. Japan, 64: 51-80. doi:10.14943/gbhu.64.51

Yamamoto H., Nakamori N., Terabayashi M., Rehman H. U., Ishikawa M., Kaneko Y. and Matsui T., 2010. Subhorizontal tectonic framework of the Horoman peridotite complex and enveloping crustal rocks. Isl. Arc, 19: 458-469. doi:10.1111/j.1440-1738.2010.00727.x

Yamamoto J., Ishibashi H., Hagiwara Y., Yokokura L. and Niida K., 2022. Raman spectroscopic identification of continuity of a channel olivine in a peridotite specimen. Geochem. Jour. 56: GJ22003. doi:10.2343/geochemj.GJ22003

Yoshida, H. and Takahashi, N., 1997. Chemical behavior of major and trace elements in the Horoman mantle diapir, Hidaka belt, Hokkaido, Japan. Jour. Mineral. Petrol. Econ. Geol., 92: 391-409. doi:10.2465/ganko.92.391

Yoshikawa M. and Nakamura E., 2000. Geochemical evolution of the Horoman peridotite complex: implications for melt extraction, metasomatism, and compositional layering. J. Geophys. Res., 105: 2879-2901. doi:10.1029/1999JB900344

Yoshikawa M., Nakamura E. and Takahashi N., 1993. Rb-Sr isotope systematics in a phlogopite-bearing spinel lherzolite and its implications for age and origin of metasomatism. J. Mineral. Petrol. Econ. Geol., 88: 121-130. doi:10.2465/ganko.88.121

Yoshikawa M., Niida K. and Green D. H., 2019. Dunite channels within a harzburgite layer from the Horoman peridotite complex, Japan. Isl. Arc, 28: e12279. doi:10.1111/iar.12279.

Received, January 26, 2026
Accepted, June 5, 2026